ChemCatChem

ChemCatChem
Chemistry Europe
European Chemical Societies Publishing

CONCEPT OPEN ACCESS

Dimethyl Ether as Circular Hydrogen Carrier: Low-Temperature Steam Reforming Over Copper–Zeolite Bifunctional Catalysts

Nick Heiming[1,2] | Chalachew Mebrahtu[1,2] | Regina Palkovits[1,2]

[1]Institute for a sustainable Hydrogen Economy, Forschungszentrum Jülich GmbH, Jülich, Germany | [2]Institut für Technische und Makromolekulare Chemie, RWTH Aachen University, Aachen, Germany

Correspondence: Regina Palkovits (palkovits@itmc.rwth-aachen.de; r.palkovits@fz-juelich.de)

Received: 3 November 2025 | **Revised:** 30 April 2026 | **Accepted:** 30 April 2026

Keywords: dimethyl ether (DME) | hydrogen | low temperature | steam reforming | zeolite

ABSTRACT

In the context of a green H_2-based economy, chemical H_2 carriers are essential for efficient H_2 storage and transportation. Among H_2 carriers, dimethyl ether (DME) is a promising candidate due to its characteristics, such as non-toxicity, easy transportation, high H_2 storage capacity, and its circular nature by the reusability of CO_2 formed from DME steam reforming (DME SR). H_2 stored in DME can be released via DME SR over a bifunctional catalyst, consisting of a solid acid and a metal-based catalyst. The reaction conditions, in particular, the reaction temperature, are crucial for an efficient H_2 release and depend on the catalysts employed. This concept paper first highlights DME synthesis by CO_2 hydrogenation and then discusses in detail the advances for DME SR at temperatures below 300°C. The kinetic and thermodynamic limitations for DME SR as well as challenges due to side reactions are presented. Zeolites are discussed as promising candidates for low-temperature applications for the DME hydrolysis step and current insights into structure–activity relationships are highlighted. Catalyst deactivation due to coking and possible regeneration strategies are presented and last, perspectives for developing optimized catalysts for low-temperature DME SR are provided.

1 | Introduction

CO_2 emissions from excessive fossil fuel use have risen strongly since 1950, leading to a rapid increase in atmospheric CO_2 concentration and global temperature rise [1]. According to the data in 2024, 38.5% of global CO_2 emissions were related to the power sector, followed by the industry (28.5%) [2]. Hence, a decrease in CO_2 emissions is necessary to slow down the rise in global temperature and the ongoing climate change. Alternatively, using green hydrogen (H_2) as fuel for energy production and industrial processes can significantly reduce CO_2 emissions [3]. Green H_2 can be produced by electrochemical water splitting, using renewable energy sources such as solar and wind power [3]. However, due to the intermittent nature of these renewable energy sources and the distant H_2 production sites, storage and transportation of green H_2 are crucial factors to implement a sustainable H_2 economy [4].

The simplest methods of H_2 transportation and storage include either compressing H_2 into gas bottles (tanks) or liquifying H_2. However, compressed H_2 gas has a low volumetric energy density and a risk of hydrogen diffusion through the container walls [5]. Moreover, the liquefaction of H_2 requires higher energy (i.e., 11.62 MJ kg^{-1}), and the volumetric energy density of liquified H_2 is lower than other liquids, for example, 8.4 MJ L^{-1} for liquid H_2 and 15.7 MJ L^{-1} for methanol [5]. Therefore, instead of storing pure H_2, using other molecules as H_2 carriers enables higher energy density and increases the H_2 storage capacity.

TABLE 1 | Volumetric energy density and technical hydrogen storage capacity of compressed H_2 and simple H_2 carrier molecules.

Hydrogen carrier	Volumetric energy density (MJ L^{-1})	Gravimetric energy density (MJ kg^{-1})	wt.%
Hydrogen, compressed	2.1[a] [5]	120[a] [5]	100
Methanol	15.7 [5]	19.7 [5]	18.8 [4]
Dimethyl ether	20.6 [9]	30.8 [9]	26.1 [4]

[a]293.15 K, 200 bar.

Examples of such organic H_2 carriers include benzyl toluene and methanol. Compared to other H_2 carriers, methanol offers the advantage of being produced by direct CO_2 hydrogenation, and the stored H_2 can be released via the steam reforming reaction [6]. However, methanol is corrosive and toxic, which complicates its storage, transport, and use in existing infrastructures. On the contrary, dimethyl ether (DME), a product of the condensation of two methanol molecules, is a non-toxic and non-carcinogenic gas. DME is less corrosive, has favorable physical properties (gaseous at ambient conditions but liquefiable under mild pressure), and is easy to handle in existing LPG infrastructure [7, 8].

For H_2 carrier molecules to be considered suitable, their H_2 storage capacity presents a major criterion. Conventionally, this storage capacity is derived by comparing the mass of H_2 stored relative to the carrier molecule mass. However, since the steam reforming process also releases additional H_2 derived from the water (steam) involved in the reaction, a more accurate method of calculating the H_2 storage capacity is required. Recently, Schühle et al. introduced the term "technical hydrogen storage capacity" ($w_{H2,\,technical}$), which considers all the hydrogen released during steam reforming (Equation 1). This includes the total amount of H_2 being released, both H_2 stored in the carrier molecule and H_2 formed from water during the reaction ($m_{H2,\,released}$) in relation to the carrier molecule itself ($m_{carrier}$) [4].

$$w_{H2,technical} = \frac{m_{H2,released}}{m_{carrier}} \quad (1)$$

The volumetric energy density and the technical hydrogen storage capacity of the compressed H_2, methanol and DME as hydrogen carriers are compared in Table 1. Although compressed H_2 achieves 100 wt.% $w_{H2,\,technical}$, it is not competitive compared to the others due to safety challenges and low volumetric energy density. In contrast, both methanol and DME yield additional H_2 from the added water (steam) during reforming, resulting in $w_{H2,\,technical}$ values of 18.8 wt.% and 26.1 wt.%, respectively [4]. Compared to methanol, DME has a higher technical H_2 storage capacity and is considered a suitable H_2 carrier due to its safety as well as simplicity in technical integration into an existing infrastructure.

Additionally, similar to methanol, DME can be directly produced by one-step CO_2 hydrogenation or via a two-step process (i.e., CO_2 to methanol and methanol to DME) using efficient catalysts. When needed, the hydrogen stored in DME can be released catalytically via a steam reforming reaction (DME SR) and used in various applications, for example, in fuel cells [10]. Steam reforming of DME releases H_2 and CO_2, and the CO_2 can be utilized as a

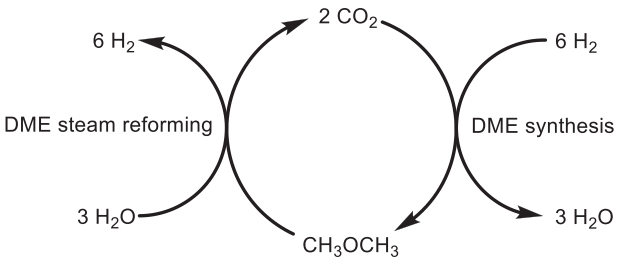

SCHEME 1 | The closed-loop CO_2-based cycle of dimethyl ether (DME) as a hydrogen carrier, illustrating DME steam reforming for H_2 production and the subsequent catalytic synthesis of DME from CO_2 and H_2, thereby enabling a circular carbon–hydrogen pathway.

$$CO_2 + 3\,H_2 \xrightleftharpoons{\text{Metal}} CH_3OH + H_2O \quad (1)$$

$$2\,CH_3OH \xrightleftharpoons{\text{Acid}} CH_3OCH_3 + H_2O \quad (2)$$

SCHEME 2 | DME synthesis: (1) Hydrogenation of CO_2 over a metal-based catalyst to form methanol and water and (2) condensation of methanol to DME and water over an acid catalyst.

feedstock for the DME synthesis. Accordingly, DME is considered a circular hydrogen carrier. The reaction cycle of DME synthesis and DME SR is shown in Scheme 1. DME SR is performed either at high temperatures (500°C) with Ni-based catalysts or at milder conditions (400°C–450°C) with Cu-based catalysts, both in combination with alumina. Although high-temperature DME SR results in high DME conversion and H_2 yield, it facilitates undesired side reactions (methane formation and C-deposition) and compromises catalyst stability [11, 12]. On the contrary, low-temperature DME SR over optimized bifunctional catalysts offers comparable H_2-yield, lower energy requirements, and improved compatibility with compact, on-board reformers, for example, for fuel cell applications.

Recent studies have focused on thermodynamic modeling and process analysis of DME SR to optimize H_2 production and predict reaction behavior. For example, Ighalo et al. developed a thermodynamic model for DME SR between 450°C and 750°C and 1–5 atm pressure to predict the formation of H_2, CO_2, CO, and CH_4 species [13]. Furthermore, thermodynamic calculations excluding methane formation showed a good agreement to experimental results [14]. This indicates that although methane formation is thermodynamically favorable, it is kinetically limited under certain experimental conditions. A reactor scale modeling developed a three-dimensional isothermal computational fluid dynamics model and compared it with experimental data using Cu–Zn/γ-Al_2O_3 as a catalyst in a temperature range between 200°C and 500°C. A high similarity of the model with the

experimental data, was observed with over 90% DME conversion and H_2 yield of over 80% at temperatures ≥400°C [15]. Not only can the reaction itself be modeled, but also the reactor system. Moreover, modeling has also been applied to reactor design and optimization. A spiral heated tubular reactor system model was validated experimentally, and demonstrated that reactor geometry significantly affects performance [16]. Compared to a conventional reformer, the optimized spiral heated reformer achieved higher DME conversion, H_2 production rate, and a higher thermal efficiency [16].

Alongside the modeling studies, catalyst design remains critical for improving performance and stability. Investigation on the effect of copper loading and γ-Al_2O_3 surface area identified 10 wt.% as optimal copper loading, and a higher γ-Al_2O_3 surface area was beneficial for reduced carbon deposition [17]. Similarly, amorphous silica–alumina composites with high amount of acidic sites and a high acid strength enhanced DME conversion and H_2 yield [18]. Moreover, alternative catalyst systems such as In_2O_3/ZrO_2 mixed with γ-Al_2O_3, showed a stable catalytic performance over 120 h at 350°C with H_2 yield of 88%, 85% CO_2 selectivity, and 13% CO selectivity [19].

As evidenced in the representative studies mentioned above, most recent studies on DME SR have focused on reactor modeling, catalyst design, and process optimization at temperatures above 300°C, with Al_2O_3 as a standard acid catalyst. This trend is reflected in the recent review articles. A comprehensive review in 2024 discussed DME reforming catalysts for steam reforming, partial oxidation, autothermal reforming, and dry reforming [20]. However, it presented almost exclusively alumina-based acid catalysts with good activity in DME SR at 350°C and above. The potential use of zeolites as acid catalysts for DME SR below 300°C was not discussed. Similarly, another review article on H_2 storage and chemical H_2 carriers discussed a limited number of studies using zeolites for low temperature DME SR at temperatures below 300°C, but primarily focused on storage and transport aspects of different hydrogen carriers rather than catalyst design and performance. Yet, only the extensive review article by Catizzone et al. (2021) on DME as a hydrogen carrier included zeolite-based acid catalysts for DME SR alongside catalysts for DME synthesis from CO_2 and H_2 and concluded that further research is required to improve DME SR performance, particularly at temperatures below 300°C [7].

Given that recent studies on DME SR predominantly focus on Al_2O_3-based acid catalyst and reaction temperatures ≥ 350°C, the potential of low temperature DME SR remains insufficiently presented. At reaction temperatures below 300°C, side reactions such as reverse water gas shift reaction or DME decomposition, that is, illustrated in Scheme 3 (3, 4), are suppressed, thereby H_2 yield is improved. Therefore, efficient catalyst design for DME SR should aim to improve DME conversion and H_2 production while minimizing CO selectivity and other side reactions. Since these undesired reactions mostly occur at high temperatures, low-temperature DME SR offers a distinct advantage. Accordingly, this concept paper focuses on low-temperature DME SR, aiming at advancing research for efficient hydrogen release under less energy-intensive operating conditions. For the full evaluation of DME as a circular H_2-carrier, practical implementations, particularly scalability to industrial scale, and operational aspects

$$CH_3OCH_3 + H_2O \xrightleftharpoons{\text{Acid}} 2\,CH_3OH \quad (1)$$

$$2\,CH_3OH + 2\,H_2O \xrightleftharpoons{\text{Metal}} 2\,CO_2 + 6\,H_2 \quad (2)$$

$$CO_2 + H_2 \xrightleftharpoons{\text{Metal}} CO + H_2O \quad (3)$$

$$CH_3OCH_3 \xrightarrow{\text{Metal}} CH_4 + CO + H_2 \quad (4)$$

SCHEME 3 | DME SR reactions and possible side reactions: (1) Hydrolysis of DME to methanol, (2) steam reforming of methanol to H_2 and CO_2, (3) reverse water gas shift reaction, and (4) DME decomposition.

such as DME and steam supply, product stream purification and CO_2 recirculation, as well as catalyst stability and regeneration, are crucial. However, to maintain an appropriate scope, this concept paper focuses on the catalyst design and reaction conditions of DME SR, with special emphasis on low temperature conditions.

For low temperature DME SR over copper–zeolite bifunctional catalysts, the balance between zeolite-catalyzed DME hydrolysis and subsequent copper-catalyzed methanol steam reforming plays a decisive role. As DME hydrolysis is equilibrium-limited, the zeolite should possess high Brønsted acidity to enhance the reaction rate, while the copper particles in the Cu-based catalyst should be highly dispersed to ensure high methanol steam reforming activity and thereby drive the equilibrium toward hydrogen production. However, both strong Brønsted acidity and the presence of copper particles also promote side reactions, including hydrocarbon formation from DME or methanol at temperatures near 300°C and CO formation via the reverse water–gas shift (RWGS) reaction. Owing to the high Brønsted acidity, catalyst deactivation in low-temperature DME steam reforming is primarily attributed to coke formation. Despite growing interest, a clear overview of the research trends and future perspectives for low temperature DME SR over copper–zeolite bifunctional catalysts is still lacking. Hence, in this concept paper, low-temperature steam reforming as a potential H_2-release strategy from DME as a circular H_2 carrier is discussed. Initially, DME synthesis via CO_2 hydrogenation with respect to catalyst design and reaction conditions is briefly highlighted. And, the concept of DME SR and its challenges are summarized with focus on kinetic and thermodynamic limitations as well as possible side reactions. Then, key advances for low-temperature DME SR are discussed with respect to the properties of bifunctional catalysts and reaction conditions. First, DME hydrolysis and its mechanism are discussed. Second, DME SR for efficient H_2 release over bifunctional catalysts (mainly Cu–zeolites) is summarized. Afterward, catalyst deactivation and regeneration methods, as well as strategies for RWGS suppression, are explained. Finally, we provide a summary and perspective focusing on future research to facilitate the application of low-temperature DME SR.

2 | DME Synthesis

Industrially, DME is produced from syngas via a two-step process: methanol synthesis followed by its dehydration to DME in a separate reactor. However, DME can also be synthesized by CO_2 hydrogenation through a two-stage reaction. First, methanol is formed by CO_2 hydrogenation over a metal-based catalyst (Scheme 2 (1)). Second, two methanol molecules are condensed

over an acid catalyst to form DME and water (Scheme 2 (2)). DME can also be synthesized in a single-stage process using one reactor and a bifunctional catalyst. Since DME synthesis involves CO_2, H_2, and water, the reverse water gas shift reaction (RWGS) is also a key side reaction. However, CO formation should be minimized to increase DME yield. Bifunctional catalysts used for DME synthesis are often a mixture of a methanol synthesis catalyst, commonly $CuO/ZnO/Al_2O_3$ (CZA), and a methanol dehydration catalyst such as alumina or zeolites [21–23].

Several factors influence DME synthesis via CO_2 hydrogenation, including the bifunctional catalyst composition (especially, the methanol synthesis catalyst), the type of reactor used, and the reaction conditions. Various parameters such as acidity, catalyst precursor concentration, catalyst additives, mixing procedures of the bifunctional catalyst, or even enhancing CO_2 hydrogenation reaction by water sorption have been reported in the literature [22, 24–27].

An exemplary study was presented by Naik et al. [21]. They explored the effect of reactor type using fixed-bed and slurry reactors with CZA as a catalyst for methanol synthesis, comparing ZSM-5 and γ-alumina as acid catalysts. With ZSM-5, higher DME selectivity (above 60%) was observed in the fixed bed reactor, whereas in the slurry reactor a higher CO selectivity was observed. For alumina, the reaction in a fixed-bed reactor resulted mainly in CO, with only small amounts of DME at 260°C. Moreover, distinct catalytic performance trends were observed during long-term time on stream (TOS). In the fixed-bed reactor, stable CO_2 conversion was achieved after 2 days of TOS, at 260°C for both bifunctional catalysts. After 4 days of TOS, CO_2 conversion reached 29% for CZA/ZSM-5 and 15% for CZA/γ-alumina. For the zeolite containing catalyst, selectivities to DME, CO, and methanol were 65%, 33%, and 2%, respectively. In contrast, the alumina containing catalyst showed negligible DME selectivity throughout; the methanol selectivity was ~40% on day 1, dropped significantly on day 2, and stabilized at ~15% on day 4, with CO selectivity reaching 82%. When the slurry reactor is used for longer TOS, a stable CO_2 conversion of 19% was obtained after 3 days for CZA/ZSM-5, while CO_2 conversion gradually declined over CZA/γ-alumina, reaching 7% after 4 days of TOS. Compared to the fixed bed reactor, a slightly lower DME, a slightly higher CO, and similarly low methanol selectivities were obtained over the CZA/ZSM-5 catalyst. On the contrary, for CZA/γ-alumina the change to the slurry reactor led to a rise in methanol selectivity to 38% and the CO selectivity was 58%, after 4 days TOS. Similar to the fixed-bed reactor, DME selectivity over the CZA/γ-alumina remained very low. Due to the high CO selectivity in all conditions, CZA/γ-alumina was likely favoring RWGS at 260°C and was not a suitable catalyst for DME synthesis from CO_2 and H_2 under these conditions. Although relatively high CO selectivity was observed in both reactor types, CZA/ZSM-5 proved to be a more suitable catalyst for DME synthesis. The fixed bed reactor appeared more suitable for DME steam reforming, since the DME selectivity was higher and CO selectivity was lower compared to the slurry reactor [21].

Beyond methanol and DME synthesis, it is also worth noting that a high acidity of the solid acid employed can lead to the formation of hydrocarbons from the intermediate methanol [28], and the mixture of copper and acidic zeolites can also catalyze the reaction of methanol to dimethoxy methane or methyl formate, depending on the copper content, copper oxidation state, and acidity of the solid acid [29].

3 | Challenges in Balancing Conversion, Stability, and Side Reactions in DME Steam Reforming

Hydrogen stored in DME can be released via a steam reforming reaction (DME SR), though it also presents some challenges. DME SR involves two consecutive reaction steps. First, DME is hydrolyzed to methanol (Scheme 3 (1)), and the resulting methanol is reacted with steam to produce H_2 and CO_2 (Scheme 3 (2)). The hydrolysis of DME is catalyzed by acidic sites, while steam reforming of methanol requires a metal functionality, typically copper. Thus, suitable bifunctional catalysts allow to perform DME SR and produce H_2. Copper is also very active for RWGS and since CO_2 and H_2 are produced during DME SR, RWGS occurs as a possible side reaction (Scheme 3 (3)) [30, 31]. Strong acidity or high temperature can lead to the formation of methane and CO as side products (Scheme 3 (4)), but high acidity can also result in coking [7, 32]. A possible side reaction when the catalyst exhibits high Brønsted acidity, especially when zeolites are used, presents the transformation of DME to hydrocarbons [33].

A kinetic study by Oar-Arteta et al. highlighted DME hydrolysis as the rate-determining step in DME SR. Compared to the subsequent methanol SR, DME hydrolysis exhibits a lower reaction rate and a higher activation energy, indicating that it kinetically limits the overall reforming process [34]. This highlights the crucial role of acidic hydrolysis function in bifunctional catalysts and suggests that insufficient hydrolysis activity can restrict overall hydrogen production, even when the methanol reforming functionality is highly active. Another kinetic study investigated DME SR over a physical mixture of $CuO–ZnO–Al_2O_3–ZrO_2$ and ZSM-5 in a temperature range of 200°C–300°C at different space velocities. Since both DME hydrolysis and methanol SR are endothermic reactions, increasing the reaction temperature enhanced DME conversion and H_2 yield [35]. At 240°C, full DME conversion and 100% H_2 yield were achieved at the lowest space velocity of 1180 mL g_{cat}^{-1} h^{-1}. At a higher space velocity of 2461 mL g_{cat}^{-1} h^{-1}, full conversion required an increased temperature of 280°C, while even higher space velocities did not allow achieving full DME conversion at 300°C. The authors attributed the incomplete DME conversion at higher space velocities to kinetic limitations, further confirming that the intrinsic rate of DME hydrolysis constrains the overall DME steam reforming process [35]. Moreover, these results demonstrate that, along with the catalysts employed, reaction conditions such as residence time are critical parameters for achieving equilibrium DME conversion.

Thermodynamically, high-temperature and low-pressure conditions are preferred for H_2 release from DME. Semelsberger et al. calculated the thermodynamic equilibrium of DME hydrolysis (i.e., methanol as the only product) and DME SR. For both reactions, a higher temperature and a higher steam-to-carbon (S/C) ratio led to increased DME conversion. Moreover, CO formation as a product of RWGS could be suppressed by a S/C ratio higher than the stoichiometric ratio and decreasing temperatures. A selection of the calculated DME conversion for

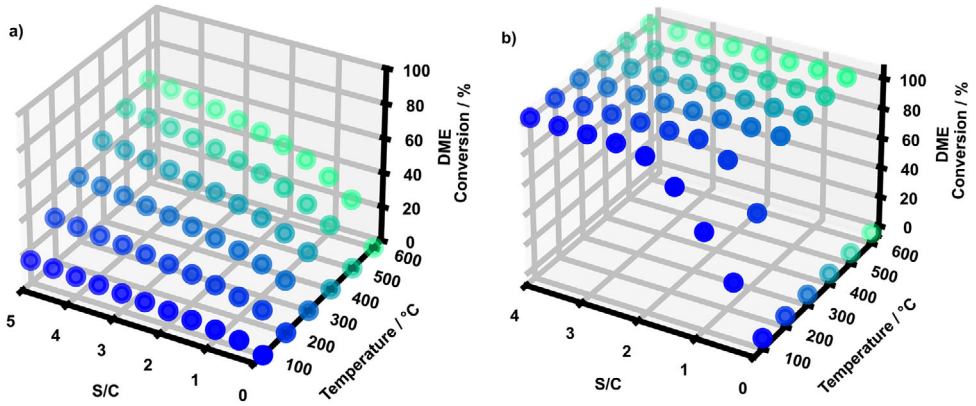

FIGURE 1 | Calculated thermodynamic equilibrium conversion on a wet basis of DME depending on the S/C ratio and the temperature for (a) DME hydrolysis and (b) DME steam reforming. DME hydrolysis is equilibrium limited even at high S/C ratios and reaction temperatures. However, DME SR can achieve full DME conversion because formed methanol is converted to H_2 and CO_2, shifting the equilibrium of DME hydrolysis to the product side. Adapted from Semelsberger et al. Copyright (2005), Elsevier [36].

both DME hydrolysis and DME SR at different S/C ratios and reaction temperatures is depicted in Figure 1 [36]. As shown in Figure 1a, the hydrolysis of DME to methanol is limited by the thermodynamic equilibrium, and DME conversion increases at higher temperatures. At a stoichiometric S/C ratio of 0.5, DME conversion increased from 4% at 100°C to 14% at 300°C, and reached 25% at 600°C. The highest DME conversion of 62% was obtained at 600°C with a S/C ratio of 5 [36]. On the contrary, DME SR is not limited by an equilibrium, as shown in Figure 1b. Full DME conversion was obtained for all conditions at temperatures above 200°C, with S/C ratios higher than 0.5. Even at 200°C and S/C ratio of 1.75, full DME conversion was achieved. H_2 formation was visualized by the H_2 production efficiency. This was determined by the calculated effluent mole fraction of H_2 divided by 0.75, since at full conversion the maximum mole fraction for hydrogen is 0.75. Despite full conversion at 200°C and above S/C ratio of 1.75, H_2 production efficiency decreased from 92.83% at 200°C to 77.23% at 600°C, which could be attributed to the RWGS reaction. At S/C ratios above 1.5, a decrease in H_2 production efficiency with increasing temperature was observed as well. Moreover, CO formation as a side product increased for DME SR with decreasing S/C ratios and increasing temperature, with maximum CO formation observed at a S/C ratio of 0.5. At this S/C ratio and a temperature range between 400°C and 600°C, the effluent mole fraction of CO was 0.3333 and H_2 was the only other product found with a mole fraction of 0.6667. When other thermodynamically viable products were also considered, methane was the most abundant one, followed by ethane and isopropyl alcohol [36].

These studies show that a slow reaction rate at temperatures below 300°C limits H_2 production during DME SR and requires appropriate adjustment of the space velocity to ensure sufficient residence time for high conversion. In particular, the kinetically limited DME hydrolysis step restricts the overall reforming rate under low temperature conditions. Furthermore, the thermodynamically unfavorable DME hydrolysis at these temperatures demands the rapid downstream conversion of the intermediate methanol to H_2 and CO_2. Continuous removal of methanol via steam reforming shifts the coupled reaction away from the DME-methanol equilibrium and toward product formation. As illustrated in Figure 1b, fast methanol conversion to H_2 and CO_2 during DME SR effectively shifts the DME hydrolysis equilibrium forward, thereby enabling high DME conversion. This highlights the importance of balancing the acid-catalyzed hydrolysis and metal-catalyzed reforming functions to achieve high overall reforming efficiency.

Copper-based catalysts are widely recognized for their high activity in methanol steam reforming. However, their thermal stability is limited by sintering at high temperatures. Operating DME SR at low temperatures would, therefore, be beneficial for maintaining catalyst stability. However, this requires that both the copper-based reforming catalyst and the acid catalyst for DME hydrolysis remain highly active at lower reaction temperatures. Spinel-type materials, such as $Cu/ZnAl_2O_4$ are well-established catalysts for methanol synthesis as well as steam reforming. In addition to this catalyst, other spinel-type materials, such as $Cu_{1.5}Mn_{1.5}O_4$, are used for DME SR. However, when $Cu/ZnAl_2O_4$ was used for DME SR without additional acid catalyst (Al_2O_3), moderate DME conversion was observed at 350°C and 400°C, increasing to above 75% at temperatures higher than 400°C [37]. The formation of H_2, CO, and CH_4 indicated that DME decomposition instead of DME SR was the dominant pathway over the spinel-type CZA catalyst without Al_2O_3. This suggests that the absence of sufficient acidic functionality limits DME hydrolysis, promoting DME decomposition at elevated temperatures. Similarly, the manganese-containing spinel without additional Al_2O_3 showed significant DME conversion only above 400°C, accompanied by substantial CH_4 formation, further confirming the dominance of the decomposition pathway in the absence of acid sites. On the contrary, the addition of acidic Al_2O_3 to both spinel-type catalysts significantly increased DME conversion and enabled selective H_2 production, demonstrating the essential role of acid sites in facilitating DME hydrolysis and enabling the coupled steam reforming pathway. The absence of methanol in the product stream indicates rapid methanol consumption, consistent with hydrolysis being the rate-determining step. Notably, while a non-spinel-type catalyst consisting of 30 wt.% Cu/Al_2O_3 exhibited a deactivation at temperatures above 400°C, the spinel-type catalysts maintained stable catalytic performance, evidencing their superior structural stability against sintering. Furthermore, for a

$CuFeMnO_4$ spinel-type catalyst combined with Al_2O_3, high S/C ratio suppressed both CO and CH_4 formation and increased CO_2 selectivity, emphasizing the importance of reaction conditions in controlling selectivity toward the desired products [37].

The above discussed study demonstrated that bifunctional catalysts combining a copper-based spinel-type with a solid acid catalyst are suitable for DME SR. The spinel-type structure improves copper stability, while the alumina as an acid component facilitates DME hydrolysis. However, Al_2O_3 as an acid showed insufficient activity below 300°C due to its limited Brønsted acidity. On the other hand, temperatures below 300°C can limit possible side reactions, but both kinetic and thermodynamic limitations of DME hydrolysis must be overcome. Zeolites, with high Brønsted acidity, can effectively promote DME hydrolysis under the low temperature conditions [38, 39]. However, their high Brønsted acidity can catalyze hydrocarbon formation at temperatures close to 300°C, reducing H_2 yield and causing coke-induced deactivation. Therefore, zeolites are a promising candidate for low-temperature DME SR, but their acidity and operation conditions must be carefully controlled to balance activity, selectivity, and stability.

4 | First Insights Into Catalyst Properties for High Performance at Low Temperature

This section focuses on recent advances in low-temperature DME SR, highlighting key studies and their mechanistic and catalytic implications. The bifunctional catalysts in this section were prepared by physically mixing the copper-based reforming catalyst with a solid acid to enable both DME hydrolysis and methanol steam reforming. As stated above, DME hydrolysis limits the overall reforming rate in DME SR; hence, a detailed understanding of the reaction mechanism is essential for the rational design and optimization of zeolite-based solid acid catalysts. The role of zeolite acid sites for DME hydrolysis was investigated by Namuangruk et al. using both experimental and computational approaches [40]. In their study, the amount of acid sites in ZSM-5 was reduced via Na-exchange from 70 μmol g^{-1} for H-ZSM-5 to 60 μmol g^{-1} for Na-ZSM-5, while maintaining comparable BET surface area and acid strength. Under similar reaction conditions, H-ZSM-5 achieved a conversion of 17%, whereas Na-ZSM-5 exhibited a slightly lower DME conversion of 15%, demonstrating the role of Brønsted acid site amount for enhanced catalytic activity. Furthermore, DME hydrolysis over H-ZSM-5 was conducted in a temperature range of 125°C–350°C to determine the apparent activation energy. Methanol formation was first observed at 150°C, increasing with reaction temperature, reaching equilibrium methanol formation at temperatures between 225°C and 300°C. At temperatures above 300°C, methanol selectivity decreased, and hydrocarbons such as CH_4, C_3H_6, and C_4H_8 were detected. This hydrocarbon formation is attributed to the high Brønsted acidity of zeolites, which promotes secondary reactions. This property is used in industry to produce gasoline and olefins [41, 42]. The experimentally determined apparent activation energy for DME hydrolysis was 76.5 kJ mol^{-1}, which was close to the calculated apparent activation energy of 75.5 kJ mol^{-1}, supporting the validity of the proposed reaction mechanism [40].

Moreover, the DME hydrolysis reaction mechanism over ZSM-5 was investigated using DFT calculations. Two possible pathways were considered: a stepwise or a concerted mechanism. Hence, the energetic profiles of the optimized structures for the mechanisms were calculated. The resulting energetic profiles of both concerted and stepwise mechanisms, including relevant atomic distances, are illustrated in Figure 2. For both mechanisms, the initial step involves the adsorption of DME at a Brønsted acid site of the zeolite. In the concerted mechanism, a water molecule coadsorbs adjacent to the DME by interacting with a neighboring oxygen. Subsequently, simultaneous demethylation and hydrolysis lead to the formation of two adsorbed methanol molecules. Lastly, the methanol molecules desorb from the zeolite, restoring the Brønsted acidic site. In contrast, the stepwise mechanism proceeds through distinct elementary steps. Following DME adsorption and protonation at the Brønsted acidic site, cleavage of a C—O bond occurs, producing one methanol molecule and a surface-bound methoxy intermediate. The methanol desorbs, while the methoxy species remains attached to the zeolite. Subsequently, a water molecule adsorbs near the methoxy group and acts as nucleophile, attacking the methoxy carbon. This hydrolysis step cleaves the methoxy–zeolite bond and forms a second methanol molecule, thereby regenerating the Brønsted acidic sites. The calculated activation barrier for the demethylation step in the stepwise DME hydrolysis mechanism was 168.8 kJ mol^{-1}, identifying it as the rate-determining step. The subsequent hydrolysis step exhibited a significantly lower activation barrier of 81.8 kJ mol^{-1}. In comparison, the concerted pathway, in which both demethylation and hydrolysis occur simultaneously, exhibited an activation barrier of 108.9 kJ mol^{-1}, which lies between the activation barriers of demethylation and hydrolysis steps in the stepwise mechanism. Therefore, it was concluded that the reaction preferably follows the pathway of the concerted mechanism [40]. These results suggest that an efficient DME hydrolysis catalyst should stabilize the transition state associated with the concerted hydrolysis pathway, while also providing sufficient accessibility for both DME and water molecules to interact with Brønsted acid sites. High Brønsted acidity can enhance DME protonation and activation, while increased water adsorption facilitates hydrolysis. It has been reported that zeolites with lower Si/Al ratios exhibit higher water adsorption capacity due to their increased hydrophilicity [43]. Additionally, lower Si/Al ratios result in a higher density of Brønsted acid sites, which can further promote catalytic activity [44]. However, excessive Brønsted acidity may also increase the possibility of hydrocarbon formation via side reactions, ultimately leading to coke formation and catalyst deactivation. Therefore, although higher acidity can enhance hydrolysis activity, catalyst design must balance acidity and stability, and lower reaction temperatures (below 300°C) may be required to minimize coke formation when highly acidic catalysts are used.

A study by Semelsberger et al. explored the effect of catalyst acidity on DME hydrolysis by evaluating various metal oxides, including alumina, zirconia, and silica, as well as ZSM-5 and Y-type zeolites with different Si/Al ratios (Figure 3). Both zeolite types were active below 300°C, and the equilibrium methanol formation was reached at 200°C. Among the tested catalysts, ZSM-5 zeolites with Si/Al ratios of 15, 25, and 40 (ZSM-5 (15), ZSM-5 (25), ZSM-5 (40)) showed the highest activity, with methanol formation initiating at temperatures as low as 150°C. In contrast,

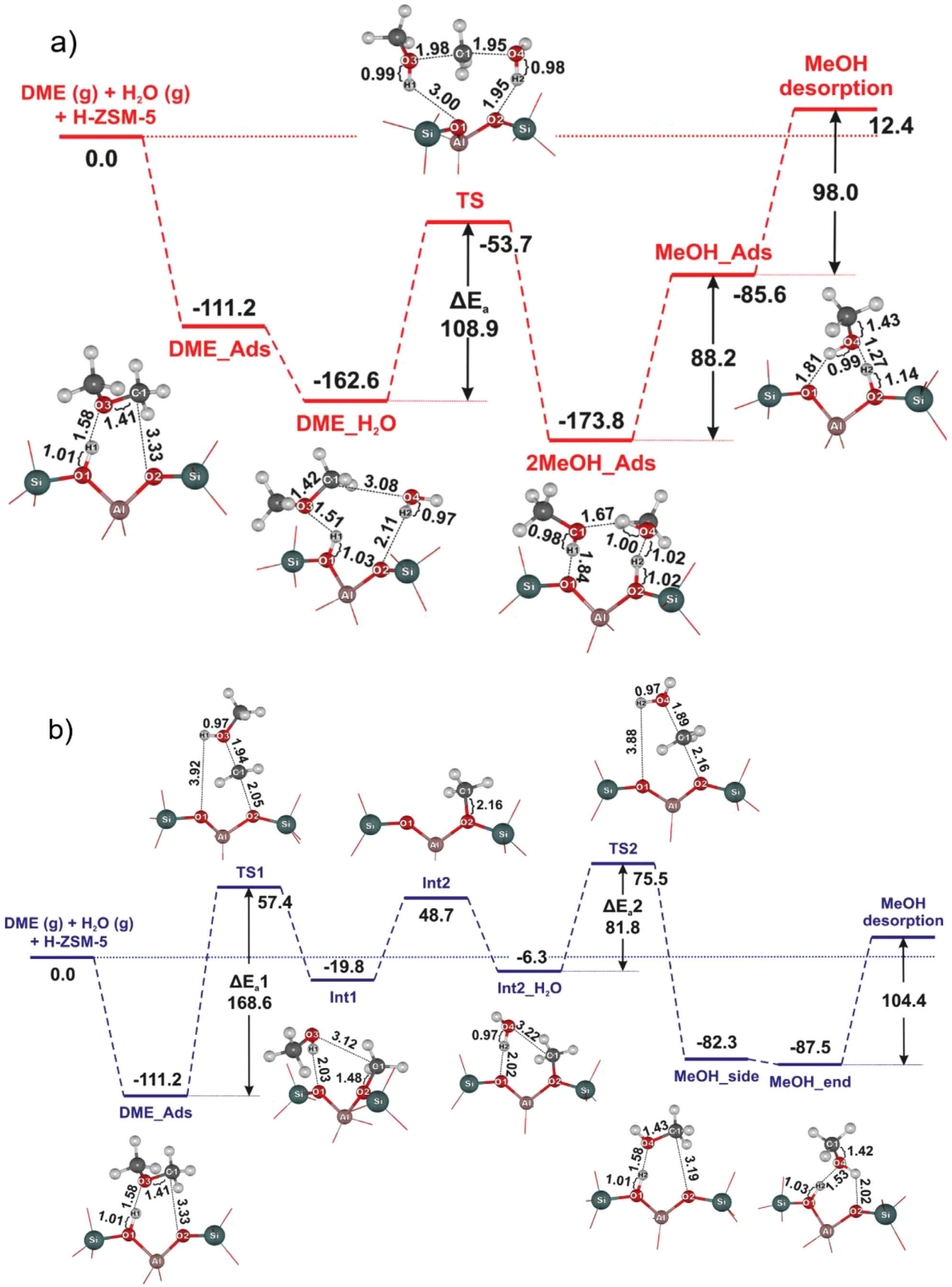

FIGURE 2 | Energetic profiles of DME hydrolysis over ZSM-5 for the (a) concerted and (b) stepwise mechanisms. The calculated apparent activation energy of DME hydrolysis was 75.5 kJ mol^{-1}, with the concerted pathway preferred due to the lower activation barrier of the demethylation-hydrolysis step. Reprinted from Namuangruk et al. Copyright (2011) American Chemical Society [40].

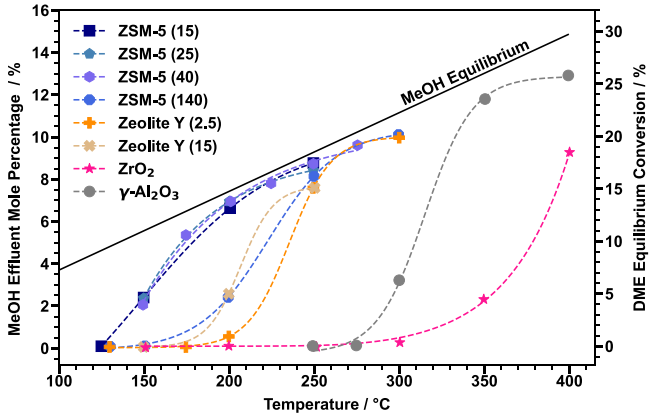

FIGURE 3 | DME hydrolysis over ZSM-5 and Y-type zeolites (Si/Al ratios in brackets), compared with alumina and zirconia. Reaction conditions: 125°C–400°C, space time = 1.00 s, S/C = 1.5. Zeolites were active for DME hydrolysis below 300°C, unlike zirconia and alumina. The high activity of ZSM-5 arises from Brønsted acidity, high surface area, Na^+ content, and hydrophobicity. Adapted from Semelsberger et al. Copyright (2005), Elsevier [45].

ZSM-5 with higher Si/Al ratio of 140 (ZSM-5 (140)) and Y-type zeolite with Si/Al of 15 (zeolite Y (15)) showed lower activity, with methanol formation occurring only from 200°C onward. Moreover, the Y-type zeolite with Si/Al of 2.5 (zeolite Y (2.5)) exhibited the lowest activity among the tested zeolites. At temperatures above 275°C, zeolites catalyze the conversion of methanol and DME to higher hydrocarbons, which limits their practicality to reaction conditions below 275°C [45].

Compared to the zeolite-based acid catalysts, alumina was active for DME hydrolysis only above 300°C, and methanol formation close to the equilibrium was only reached at 350°C. In contrast, silica showed no catalytic activity for DME hydrolysis at all reaction temperatures investigated. Zirconia, another active non-zeolite catalyst, began to form methanol at 350°C; however, equilibrium methanol formation was not achieved even at 400°C. In summary, zeolites demonstrated significantly higher activity at temperatures below 300°C compared to alumina and zirconia. Notably, methanol formation was already observed at 150°C for ZSM-5 type zeolites with a low Si/Al ratio [45].

Since DME hydrolysis is only one step in the overall DME SR reaction, Faungnawakij et al. experimentally investigated the role of acidity in DME SR by combining a Cu-based spinel catalyst active for MeOH SR with different solid acids responsible for DME hydrolysis [46]. The solid acid catalysts included commercially available alumina, H-mordenite, and ZSM-5 zeolites. To remain within the scope of low-temperature DME SR, only catalysts active below 300°C are discussed here; only alumina is included for comparison. To ensure proximity between the two components, the solid acid and $CuFe_2O_4$ were physically mixed and pressed into pellets, forming a bifunctional catalyst with better interfacial contact. Table 2 summarizes an overview of the catalysts tested in the DME SR, along with their characterization results, including BET surface area, pore volume, and acid site amount and strength. DME conversion, H_2 production, and CO selectivity of DME SR over bifunctional catalysts containing zeolites are shown in Figure 4, where results for ALO8 are included for comparison.

Commercial zeolites with high acid strength and Brønsted acid sites, when physically mixed with $CuFe_2O_4$, enabled DME conversion to H_2 at temperatures as low as 200°C, confirming the essential role of acid sites in initiating DME hydrolysis. The H-mordenite catalysts ZHM20 and ZHM90 (Si/Al ratios of 10 and 45, respectively) showed high H_2 production between 225°C and 275°C; however, it significantly declined above 300°C, although DME conversion over ZHM90 continued to increase. This indicates a shift in reaction selectivity rather than a loss of overall DME conversion. In contrast, Z5-90H maintained higher H_2 production at 300°C, although its H_2 production also decreased at higher temperatures. The decline in H_2 production above 300°C is attributed to the formation of hydrocarbons, such as C_3H_8 and C_4H_{10}, which were detected in the product gas stream [46]. This suggests that at elevated temperatures, Brønsted acid sites increasingly promote side reactions such as DME dehydration, oligomerization, and hydrogen transfer, reducing selectivity toward DME SR products. Therefore, while DME conversion may remain high, H_2 yield decreases due to competing hydrocarbon formation pathways. At temperatures below 300°C, the mordenite type zeolites showed the highest H_2 production, indicating superior performance in the optimal temperature range for low temperature DME SR (250°C–275°C). At higher temperatures, however, the increased tendency for hydrocarbon formation over strong Brønsted acid sites reduces H_2 selectivity and limits overall reforming efficiency. Separate DME hydrolysis experiments showed that the zeolites were active over the same temperature range as in DME SR, confirming that hydrolysis is not the rate-limiting step under these conditions [46]. Moreover, the hydrolysis activity of the two mordenite and the ZSM-5 zeolite was consistent with previous findings by Semelsberger et al., where equilibrium DME conversion was achieved between 200°C and 300°C for zeolites with a low Si/Al ratio [45].

This significant difference in activity during methanol formation in the study by Semelsberger et al. (Figure 3) is primarily related to the nature and amount of acidic sites. In particular, Brønsted acidity plays a decisive role in facilitating DME hydrolysis at lower temperatures. To investigate acidity, the authors performed temperature programmed surface reactions using isopropyl amine as a probe molecule to quantify both the total amount of acid sites and the Brønsted acid sites. As shown in Figure 5, a higher Si/Al ratio led to a decline in Brønsted acidity for both ZSM-5 and Y-type zeolite. In contrast, silica exhibited no measurable acidity, while alumina and zirconia possessed only low amount of Brønsted acidity [45]. Despite its low Brønsted acidity, alumina showed significant methanol formation at temperatures above 300°C. This behavior can likely be attributed to the presence of Lewis acid sites and their interaction with adsorbed water. A study on water adsorption on alumina surfaces has shown that water promotes the formation of surface hydroxyl groups. However, these hydroxyl groups do not necessarily contribute to catalytic activity at lower temperatures, as hydrogen-bonded water molecules can shield the hydroxyl groups and inhibit their participation in acid catalyzed reactions. Only at higher temperatures, excess adsorbed water is removed, exposing reactive surface hydroxyl groups capable of participating in DME hydrolysis [47]. Furthermore, a study on the catalytic behavior of Al_2O_3 for DME

TABLE 2 | Results from N_2 physisorption, acid properties of the employed catalysts, and Si/Al ratio of zeolites.

Catalyst	BET ($m^2\ g^{-1}$)	Acid amount ($\mu mol\ g^{-1}$)	Acid-site strength	Total pore volume ($cm^3\ g^{-1}$)	Si/Al ($mol\ mol^{-1}$)	Catalyst type	Referred as
$CuFe_2O_4$	1	3	—	—		Spinel oxide	
JRC-ZHM20(5)	306	720	Weak, strong	0.17	10	Zeolite-H mordenite	ZHM20
JRC-ZHM90(1)	435	260	Strong	0.54	45	Zeolite-H mordenite	ZHM90
JRC-Z5-90H(1)	347	70	Medium	0.47	45	Zeolite-MFI (ZSM-5)	Z5-90H
ALO8	141	50	Medium	1.18		Alumina-γ-Al_2O_3	

Adapted from Faungnawakij et al. Copyright (2006), Elsevier [46].

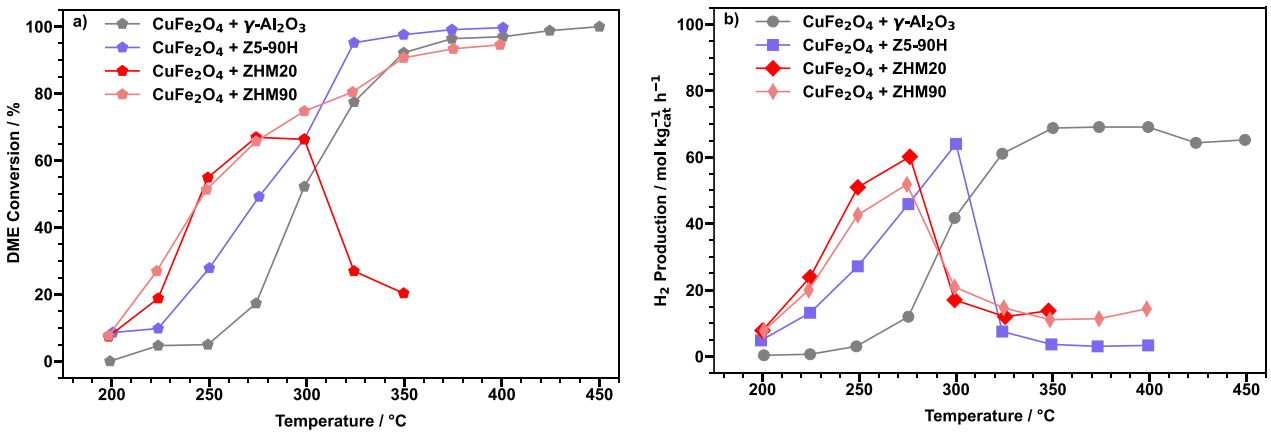

FIGURE 4 | DME SR over different zeolites and $CuFe_2O_4$ spinel: (a) DME conversion and (b) H_2 production. Reaction conditions: 200°C–400°C, gas hourly space velocity (GHSV) = 2200 h^{-1}, S/C = 1.5. Above 300°C, H_2 production decreased despite increasing DME conversion. Between 200°C and 275°C, mordenite-type zeolites outperformed ZSM-5. Adapted from Faungnawakij et al. Copyright (2006), Elsevier [46].

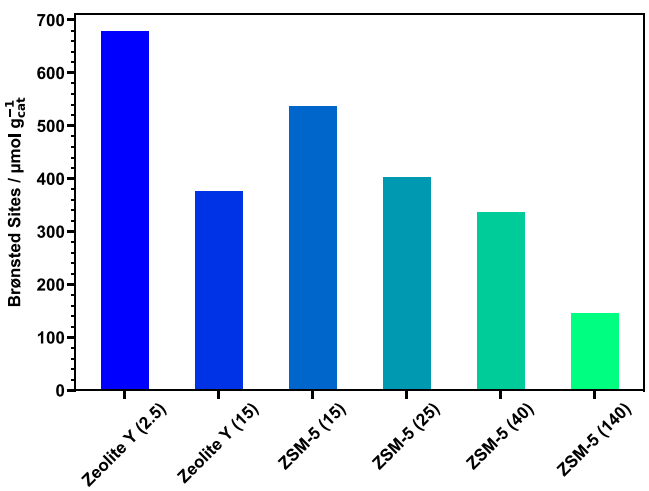

FIGURE 5 | Brønsted acidity of zeolites with varying Si/Al ratios (in brackets), determined by temperature programmed reaction of isopropyl amine. Brønsted acidity decreased with increasing Si/Al ratio. Adapted from Semelsberger et al. Copyright (2005), Elsevier [45].

hydrolysis identified these surface hydroxyl groups as active sites for DME hydrolysis [48]. This explains why DME hydrolysis, and consequently DME SR, requires reaction temperatures above 300°C when alumina is used as an acid catalyst.

When comparing the zeolites, zeolite Y (2.5) exhibited the highest amount of Brønsted sites but showed only minimal methanol formation. According to the mechanism discussed earlier, DME hydrolysis occurs on Brønsted acid sites. Therefore, a higher amount of Brønsted sites would be expected to enhance hydrolysis activity and lower the onset temperature. However, contrary to this expectation, zeolite Y (2.5) displayed the highest onset temperature for DME hydrolysis. This indicates that the amount of Brønsted sites alone does not determine the hydrolysis activity. At 250°C, the MeOH concentration measured over zeolite Y (2.5) was similar to that of zeolite Y (15), although still slightly lower than that observed for ZSM-5 zeolites.

The zeolites used in the study by Faungnawakij et al. (Figure 4) possessed strong or medium acidic sites as determined by NH_3-TPD, while alumina showed only medium acid strength. However, the measured acid site amount for ZSM-5 was significantly lower than reported by Semelsberger et al., despite a comparable Si/Al ratio (i.e., 70 $\mu mol\ g^{-1}$ Si/Al ratio of 45 vs. 336 $\mu mol\ g^{-1}$ for Si/Al ratio of 40). This discrepancy is likely due to differences in acidity characterization methods, highlighting the sensitivity of measured acid site amount to experimental conditions and analysis techniques. The presence of Brønsted acid sites in zeolites appears essential for enabling DME hydrolysis at lower temperatures and is, therefore, critical for efficient low-temperature DME SR. In contrast, the absence of strong Brønsted

acidity in alumina limits its hydrolysis activity under these conditions. Compared to the study by Semelsberger et al., a decrease in acid sites for mordenite and ZSM-5 type zeolites also results in lower DME conversion and H_2 yield at temperatures up to 275°C. However, this trend was not observed for DME hydrolysis over zeolite Y, where the zeolite Y (2.5) with higher amount of acid sites exhibited lower DME conversion. Similarly, ZSM-5 with a Si/Al ratio of 15–40 showed very similar DME conversion despite expected differences in acidity. These results indicate that Brønsted acidity alone does not govern DME hydrolysis and SR performance; additional catalyst properties also play a crucial role.

The Si/Al ratio not only affects the acidity of the zeolite but also the surface area. For both ZSM-5 and mordenite-type zeolites, increasing the Si/Al ratio led to a higher surface area. However, a high surface area alone does not necessarily translate into high DME conversion. This is evident for zeolite Y, which has a surface area above 700 $m^2\ g^{-1}$ but showed lower DME conversion than ZSM-5. Similar to acidity, surface area is only one of several factors influencing catalytic activity. Zeolite Y possesses a larger pore system than ZSM-5, which in principle should facilitate molecular diffusion and adsorption. Nevertheless, ZSM-5 with a low Si/Al ratio exhibited higher catalytic activity for DME hydrolysis than Y-type zeolites, despite its smaller pore structure. The superior low temperature performance of mordenite can be partly explained by its pore structure. According to the zeolite structures database [49], mordenite-type zeolites have a two-dimensional pore system (with a ring opening > 3.4 Å) with only one pore channel accessible to DME (kinetic diameter ≈ 4.3 Å) [50]. This restricted diffusion may increase the DME residence time within the pores, enhancing interaction with Brønsted acid sites and facilitating hydrolysis. In contrast, ZSM-5 has a three-dimensional pore system that may facilitate faster diffusion and shorter residence times, potentially reducing effective contact with active sites. Additionally, the higher acidity of ZHM20 compared to ZHM90 explains its higher H_2 production, as a higher amount of Brønsted acid sites enhances the rate of DME hydrolysis and supports higher overall reforming activity. The topology of the zeolites may be an important factor in DME hydrolysis, since a pore system close in size to the kinetic diameter of DME resulted in a higher DME conversion compared with zeolites with larger pores.

In addition to acidity and topology, structure-independent properties could have an effect on DME SR as well [45]. In the study of different zeolites for DME hydrolysis by Semelsberger et al. a significant difference between the zeolites is observed in the Na^+ content. Zeolite Y (2.5) contains substantially higher Na^+ concentration (484 μmol g_{cat}^{-1}) compared to zeolite Y (15) (32 μmol g_{cat}^{-1}), while the ZSM-5 zeolites contain only 13 μmol g_{cat}^{-1} of Na^+. Previous studies on water adsorption in ZSM-5 zeolites have shown that water molecules preferentially interact with extra-framework cations such as Na^+. At lower water partial pressures, water molecules bound directly to those cations, while at higher pressures, water clusters were formed [51]. This phenomenon likely also applies to Y-type zeolites. Consequently, the high Na content in zeolite Y (2.5) may strongly bind water molecules to Na cations rather than allowing them to interact effectively with Brønsted acid sites. Since water is a reactant in DME hydrolysis, this competitive adsorption could reduce the availability of water at the active Brønsted acid sites and delay the onset of hydrolysis, resulting in lower activity despite the higher amount of Brønsted acid sites. For the ZSM-5 zeolites, ZSM-5 (15), ZSM-5 (25), and ZSM-5 (40) exhibited decreasing acidity and increasing surface area with increasing Si/Al ratio, yet showed similar DME hydrolysis performance. This suggests that neither acidity nor surface area alone fully explains the observed activity trends in DME hydrolysis. Hydrophobicity may also play a role, as literature reports that the hydrophobicity of HZSM-5 increases with increasing Si/Al ratio [52]. In principle, higher hydrophobicity would reduce water adsorption and thus decrease the DME hydrolysis rate. However, this effect was not observed for ZSM-5 with a Si/Al ratio below 100. It is likely that within this relatively low Si/Al range, the change in hydrophobicity is insufficient to significantly influence water adsorption or DME hydrolysis activity. As a result, the DME hydrolysis rates remain similar across these ZSM-5 zeolites despite the difference in acidity and surface area.

In addition to the above-discussed ZSM-5, mordenite- and Y-type zeolites, more zeolite types were tested for DME hydrolysis and, when mixed with $CuFe_2O_4$ spinel, also for DME SR, including beta (BEA), ferrierite (FER), and L-type (LTL) zeolites [53]. All the zeolites were calcined at 500°C for 0.5 h, and their acidity was characterized by NH_3-TPD before and after calcination. Although the total measured acidity for all samples reduced after calcination, no quantitative values were reported, which limits a rigorous comparison of acidity loss and its correlation with catalytic performance. After calcination, LTL showed the highest amount of NH_3 adsorbed, followed by FER, while MOR and FAU exhibited intermediate NH_3 adsorption, and BEA and ZSM-5 (MFI) showed the lowest. In contrast, FAU showed the highest surface area, followed by BEA and MFI, whereas MOR and LTL had slightly lower but comparable surface areas, and FER had the lowest surface area among the calcined zeolites. A similar trend was observed after mixing the zeolites with $CuFe_2O_4$.

In terms of catalytic performance, BEA and FER showed a similar DME hydrolysis activity up to 250°C, while MOR exhibited a comparable activity up to 200°C. At temperatures above 300°C, BEA and MFI showed an apparent DME conversion exceeding equilibrium, which likely resulted from parallel side reactions such as hydrocarbon formation that irreversibly consume DME and increase the measured conversion beyond the equilibrium limit for DME hydrolysis to methanol. Despite their relatively high NH_3 adsorption capacity, LTL and FAU showed the lowest DME conversion of all tested zeolites between 150°C and 300°C. Notably, none of the zeolites achieved equilibrium DME conversion under the investigated conditions, in contrast to previous studies where MFI, MOR, and FAU achieved equilibrium conversion, suggesting possible differences in experimental conditions, catalyst pretreatment, or mass transport limitations that were not addressed. Overall, the results indicate that while calcination influences acidity and may improve catalyst stability, the catalytic performance in DME hydrolysis depends on a complex interplay of acidity, pore structure, and diffusion effects, and the absence of quantitative acidity data and site-normalized activity limits the strength of structure–activity correlations.

During DME SR, all zeolites mixed with $CuFe_2O_4$ could produce H_2. DME conversion and H_2 production over the bifunctional

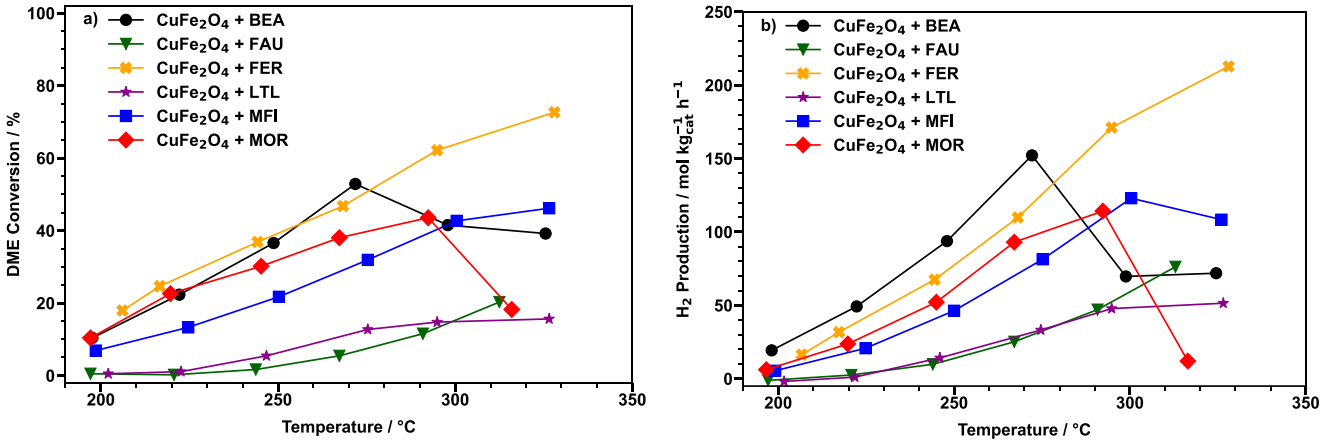

FIGURE 6 | DME SR over bifunctional catalysts ($CuFe_2O_4$ + zeolites). (a) DME conversion and (b) rate of H_2 production. Reaction conditions: 200°C–325°C, W/F = 5.0 g min L^{-1}, S/C = 2.5. Catalysts with beta- and ferrierite-type zeolites showed the highest DME conversion and H_2 production, consistent with their high DME hydrolysis activity. Adapted from Shimoda et al. Copyright (2011), Elsevier [53].

catalysts during DME SR are shown in Figure 6. Similar to DME hydrolysis, the bifunctional catalysts containing FAU and LTL zeolites showed low DME conversion and H_2 production, which only started at 240°C. In contrast, the other bifunctional catalysts showed a higher DME conversion and H_2 production at these temperatures. A similar trend was observed for these catalysts, that is, an increase in H_2 production with rising temperatures until 300°C. Interestingly, DME conversion and H_2 production continued to increase further at 300°C and above over the bifunctional catalyst containing FER, whereas the catalysts containing BEA, MFI, and MOR zeolites exhibited declining H_2 production above 300°C. In comparison, the bifunctional catalyst containing FER showed the highest DME conversion and H_2 production at 325°C [53]. When looking at the H_2 production below 300°C, the bifunctional catalyst containing BEA, FER, and MOR showed the highest activity, followed by MFI. These zeolites also showed the highest activity for DME hydrolysis. Since the same Cu-based catalyst was used in all reactions, the observed difference in reactivity was mostly attributed to the zeolite component and, consequently, to its influence on the DME hydrolysis step. However, mixing $CuFe_2O_4$ with the zeolite also affected the reduction behavior of copper. The reduction temperature shifted from 385°C for $CuFe_2O_4$ + LTL to 380°C for FER and to 375°C for MFI and MOR. The mixing with BEA and FAU lowered the reduction temperature further to 345°C, indicating improved Cu dispersion in these bifunctional catalysts. Higher dispersion of metallic copper is generally considered beneficial for the steam reforming reaction due to the increased availability of active sites [53]. Consistent with this, BEA mixed with $CuFe_2O_4$ showed the highest rate of H_2 production, which was in agreement with its lower reduction temperature and high activity for DME hydrolysis. In contrast, although the bifunctional catalyst based on FAU had the same reduction temperature as BEA, it exhibited the lowest activity for DME SR. This discrepancy is most likely due to the low intrinsic activity of FAU for DME hydrolysis, which limits the formation of intermediate species required for the subsequent steam reforming step, highlighting that efficient DME hydrolysis is essential for high overall DME steam reforming activity. The bifunctional catalysts containing MFI and MOR showed a lower H_2 production than the one containing BEA, which could be attributed to the higher reduction temperature of 375°C. At temperatures around 200°C, DME conversion during DME hydrolysis and DME SR for MOR was similar to BEA, but lower H_2 production was observed. This is another indicator that the reduction temperature and, therefore, Cu dispersion is crucial for the steam reforming step. BEA exhibited the second lowest NH_3 adsorption; however, the best results for DME hydrolysis and DME SR were achieved by the catalyst containing BEA. LTL, on the other hand, showed significantly worse H_2 production despite having the highest adsorption of NH_3. This indicates that not only the acidity itself but also other properties like the pore structure and accessibility of the acid sites are important for DME hydrolysis. This study demonstrated that, beyond zeolite properties such as acidity and topology, it is important to consider the interplay between the acidic functionality and the Cu-based catalyst. In particular, the reduction behavior and dispersion of Cu, factors not addressed in the previously discussed studies, have a significant impact on the overall performance.

Not only can zeolites perform low-temperature DME SR, but also heteropoly acids like 12-tungstosilico heteropoly acid ($H_4SiW_{12}O_{40}$) are active for DME hydrolysis between 200°C and 300°C. $H_4SiW_{12}O_{40}$ on alumina can hydrolyze DME to methanol in this temperature range, and at 300°C, both DME conversion and methanol formation reach thermodynamic equilibrium. Even at 340°C, DME conversion remains at equilibrium. Methanol steam reforming using a Cu/SiO_2 catalyst achieves full methanol conversion at 280°C with low CO levels. The activity of the bifunctional catalyst in a 1:1 weight ratio for DME SR was very low at 220°C, but as the temperature increased, DME conversion and H_2 production rose until complete conversion was observed at 290°C. At 290°C, CO concentration was below 5 vol.%, with H_2 and CO_2 being the only products detected, and no other side products were observed [54]. Since no characterization of the heteropoly acid or Cu/SiO_2 was given, a comparison of the acidity or the presence of Brønsted or Lewis acid sites with the aforementioned zeolites is not possible. But the fact that only CO as a side product was detected indicates that the acid sites did not participate in the formation of hydrocarbon, as seen for zeolites. Further investigation of the acid sites in heteropoly acids is necessary to determine the reason

for the absence of other side reactions other than RWGS reaction that contributed to the CO selectivity.

5 | Catalyst Deactivation and Regeneration

The bifunctional catalyst for DME SR is susceptible to deactivation due to the combined effects of the Brønsted acidity of zeolites and the intrinsic instability of copper under reaction conditions. The Brønsted acid sites in zeolites promote hydrocarbon formation, which can result in carbon deposition (coking) and blockage of active sites. In parallel, copper particles are prone to sintering at elevated temperatures, leading to a loss of active surface area and reduced catalytic activity. Consequently, catalyst deactivation is likely during longer time on stream. The mechanisms of catalyst deactivation and strategies for regeneration have been investigated in several studies. One approach to improve the stability of Cu-based catalysts involves the formation of spinel-type structures, which enhance resistance to sintering. For example, compared to Cu/SiO_2 catalyst, SiO_2 supported $CuFe_2O_4$ spinel (calcined at 800°C) showed a high H_2 production with no apparent deactivation during methanol steam reforming. Besides, even after deliberate sintering of Cu by H_2 reduction at 600°C, the spinel-type catalyst could be regenerated by calcination at 800°C, highlighting its regenerative potential and structural robustness [55].

In the previously discussed study by Faungnawakij et al., the side products of DME hydrolysis over zeolites at 350°C were analyzed. At elevated temperatures, the main side products were hydrocarbons (C_3H_8 and C_4H_{10}) with a concentration of 14.7 – 17.3% in the product stream, whereas methane was only formed in small fractions (0.9%–2.3%) [46]. The formation of these hydrocarbons, combined with the observation that DME conversion over highly acidic mordenite decreased significantly at temperatures above 300°C, indicates progressive catalyst deactivation due to coke formation. Furthermore, the formation of hydrocarbons and catalyst deactivation at 300°C and above is consistent with the other studies as well. In the following two studies, heat treatment has been investigated both as a possible regeneration strategy after the catalyst deactivation and as a pretreatment condition to enhance resistance to coking [53, 56]. The findings of these studies are summarized in Table 3.

In addition to heat treatment, Shimoda et al. investigated a bifunctional catalyst consisting of ZSM-5 mixed with $CuFe_2O_4$ spinel and its deactivation during DME SR [56]. Coke formation was identified as the primary cause of catalyst deactivation. However, increasing the $CuFe_2O_4$ spinel to zeolite ratio from 1/1 to 8/1, combined with increasing the S/C ratio from 2.0 to 3.5, suppressed deactivation. With a $CuFe_2O_4$ spinel to zeolite ratio of 8/1, no apparent deactivation was observed over 20 h TOS. Furthermore, increasing the S/C ratio extended the duration of H_2 production above 50 mol kg_{cat}^{-1} h^{-1} from less than 5 h to approximately 7.5 h TOS. The higher water content probably suppressed the hydrocarbon formation pathway, but in these harsh conditions, it is also likely that copper is being oxidized, reducing the H_2 production. The higher stability at higher spinel/zeolite ratios might be caused by an abundance of copper, so that the oxidation of some part of the copper did not diminish the activity for steam reforming. The catalyst could also be regenerated by thermal treatment at high temperatures, indicating that deactivation was largely reversible and associated with coke deposition. However, due to the thermal treatment, the spinel structure could also be regained, thereby restoring the activity. The $CuFe_2O_4$ spinel and ZSM-5 mixture showed increasing DME conversion and H_2 production between 200°C and 300°C. However, at reaction temperatures above 300°C, H_2 production decreased while DME conversion remained unaffected. This trend suggests that side reactions became more dominant at higher reaction temperatures. In particular, hydrocarbons such as C_2H_4, C_2H_6, and C_3H_8 were detected in the product stream, indicating that the zeolite promoted hydrocarbon formation via acid-catalyzed reactions rather than facilitating DME hydrolysis under these reaction conditions [56].

Due to the observed catalyst deactivation caused by coking, heat treatment in air of the spent catalyst was studied as a possible regeneration strategy (Figure 7c). Regeneration at 300°C restored the initial activity of the catalyst, but it deactivated faster than the untreated catalyst. And, the H_2 production over the regenerated catalyst remained low but was still present after the decline in activity, while the untreated catalyst showed almost no H_2 formation. After treatment at 500°C and 700°C, the deactivated catalyst not only recovered activity to the level of the fresh catalyst but also exceeded the original activity. The H_2 production over these regenerated catalysts was also very stable throughout the 20 h reaction time, and enhanced H_2 production was observed after regeneration at 500°C compared to regeneration at 700°C. The catalyst was regenerated by burning off the carbon deposits and it might be that the acidity of the zeolite was recovered by this treatment.

The authors also found that after steam reforming, metallic copper was present, which is considered to be the active species for methanol SR. The copper was probably reduced by either the formation of H_2 or CO during the initial phase of the reaction. A high regeneration temperature led to migration of copper into the spinel structure and at a regeneration temperature of 900°C, the $CuFe_2O_4$ spinel phase was fully restored. The regeneration at 300°C, 500°C, and 700°C did not result in the full regeneration of the $CuFe_2O_4$ spinel, but different $Cu_xFe_{3-x}O_4$ phases were found [56]. Unfortunately, the authors did not investigate the acidity of the zeolite after this regeneration treatment. The heat treatment could alter the zeolite acidity, either reducing the amount of acid sites or reducing the acid strength and, therefore, could reduce the zeolite's activity for hydrocarbon formation and could lower the amount of carbon deposition, prolonging the catalyst life. It was also found that after regeneration at 500°C and 700°C, CuO grains smaller than the grains of the as-prepared catalyst were dispersed on the surface of the remaining Fe_2O_4 spinel [56]. After reduction, these highly dispersed CuO grains would result in highly dispersed metallic copper particles and could cause the higher activity observed in Figure 7c. When the catalyst was regenerated at 900°C, a stable H_2 production similar to the fresh catalyst was achieved after a short induction period. The induction period was not observed for the other regenerated catalysts and could be attributed to a lower reducibility of copper after the treatment at 900°C and the restoration of the original spinel structure. Similar to the spent samples of the fresh catalysts, TPO was performed over the regenerated catalysts after the reaction to determine coke deposition. Compared to the

TABLE 3 | Reaction conditions, H_2 production, and catalyst deactivation of DME SR using $CuFe_2O_4$ + ZSM-5 (Si/Al: 45) with 2/1 weight ratio as a catalyst.

Reaction conditions	Treatment	Initial H_2 production (mol kg_{cat}^{-1} h^{-1})	Deactivation	References
300°C W/F: 3.0 g min L^{-1} S/C: 2.5	As prepared	~190	Decline in H_2 production after first hour TOS, loss of H_2 production after 7.5 h TOS	[56]
300°C W/F: 3.0 g min L^{-1} S/C: 2.5	Regeneration in air at 300°C	~190	Decline in H_2 production after first hour TOS, below 50 mol kg_{cat}^{-1} h^{-1} after 3 h TOS	[56]
300°C W/F: 3.0 g min L^{-1} S/C: 2.5	Regeneration in air at 500°C	~250	No deactivation in 20 h TOS observed	[56]
300°C W/F: 3.0 g min L^{-1} S/C: 2.5	Regeneration in air at 700°C	~225	No deactivation in 20 h TOS observed	[56]
300°C W/F: 3.0 g min L^{-1} S/C: 2.5	Regeneration in air at 900°C	~190	No deactivation in 20 h TOS observed	[56]
325°C W/F: 5.0 g min L^{-1} S/C: 2.5	As prepared	~110	Decline in H_2 production after first hour TOS, below 50 mol kg_{cat}^{-1} h^{-1} after 2.5 h TOS	[53]
325°C W/F: 5.0 g min L^{-1} S/C: 2.5	Calcined before DME SR in air at 300°C	~190	Loss of H_2 production after 5 h TOS	[53]
325°C W/F: 5.0 g min L^{-1} S/C: 2.5	Calcined before DME SR in air at 500°C	~190	Loss of H_2 production after ~7.5 h TOS	[53]
325°C W/F: 5.0 g min L^{-1} S/C: 2.5	Calcined before DME SR in air at 700°C	~190	Loss of H_2 production after ~9 h TOS	[53]
325°C W/F: 5.0 g min L^{-1} S/C: 2.5	Calcined before DME SR in air at 900°C	~190	Loss of H_2 production after 5 h TOS	[53]

All reactions were conducted for 20 h TOS, no CO selectivity, and DME conversion were reported. Catalyst deactivation was attributed to coking. The values are taken from figures in the original publications [53, 56].

untreated and the at 300°C regenerated catalysts, the amount of coke on the catalysts that were regenerated at 500°C, 700°C, and 900°C was lower [56]. The lower coke deposition was most likely caused by a lower acidity, most likely a lower amount of acid sites due to the heat treatment. Because less acid sites were available, DME hydrolysis was the preferred reaction over hydrocarbon formation, leading to less coking. The H_2 production of the at 900°C regenerated catalyst was very similar to the H_2 production seen in Figure 7b, as both reactions were performed at 300°C. This might be due to the restoration of the original $CuFe_2O_4$ spinel structure and, therefore, similar activity for DME SR. It seemed that the poor stability of the catalyst at 300°C could be improved by re-calcining and thereby restoring the spinel structure. With these findings in mind, a future research approach would be to investigate whether the H_2 production remains stable for even longer TOS or whether a reduction and subsequent re-calcination at 500°C or 700°C before conducting DME SR would produce a more stable catalyst and would prevent catalyst deactivation in the first place.

In the study by Shimoda et al. (2011), catalyst pretreatment conditions prior to the DME SR were investigated to improve stability [53]. Thermal pretreatment of ZSM-5 mixed with $CuFe_2O_4$ at 900°C led to a higher stability during DME SR at 325°C compared to the untreated catalyst (Figure 7d). Calcining the $CuFe_2O_4$/ZSM-5 mixture catalyst prior to DME SR most likely reduced catalyst deactivation, enabling stable H_2 production for over 10 h TOS. Calcination at 700°C also improved stability, maintaining stable H_2 production for up to 10 h TOS. On the contrary, the untreated catalyst showed fast deactivation within the first hour on stream [53]. These results indicate that high temperature calcination reduces catalyst deactivation, most likely by decreasing coke formation or altering the physicochemical properties of the catalyst, such as acidity, metal dispersion, or metal–support interaction. The same catalyst mixture was also investigated in a previous study (Figure 7a–c), where higher productivity was observed, particularly after regeneration at 500°C and 700°C, compared to the results shown in Figure 7d. On one hand, differences in reaction conditions, such as reaction

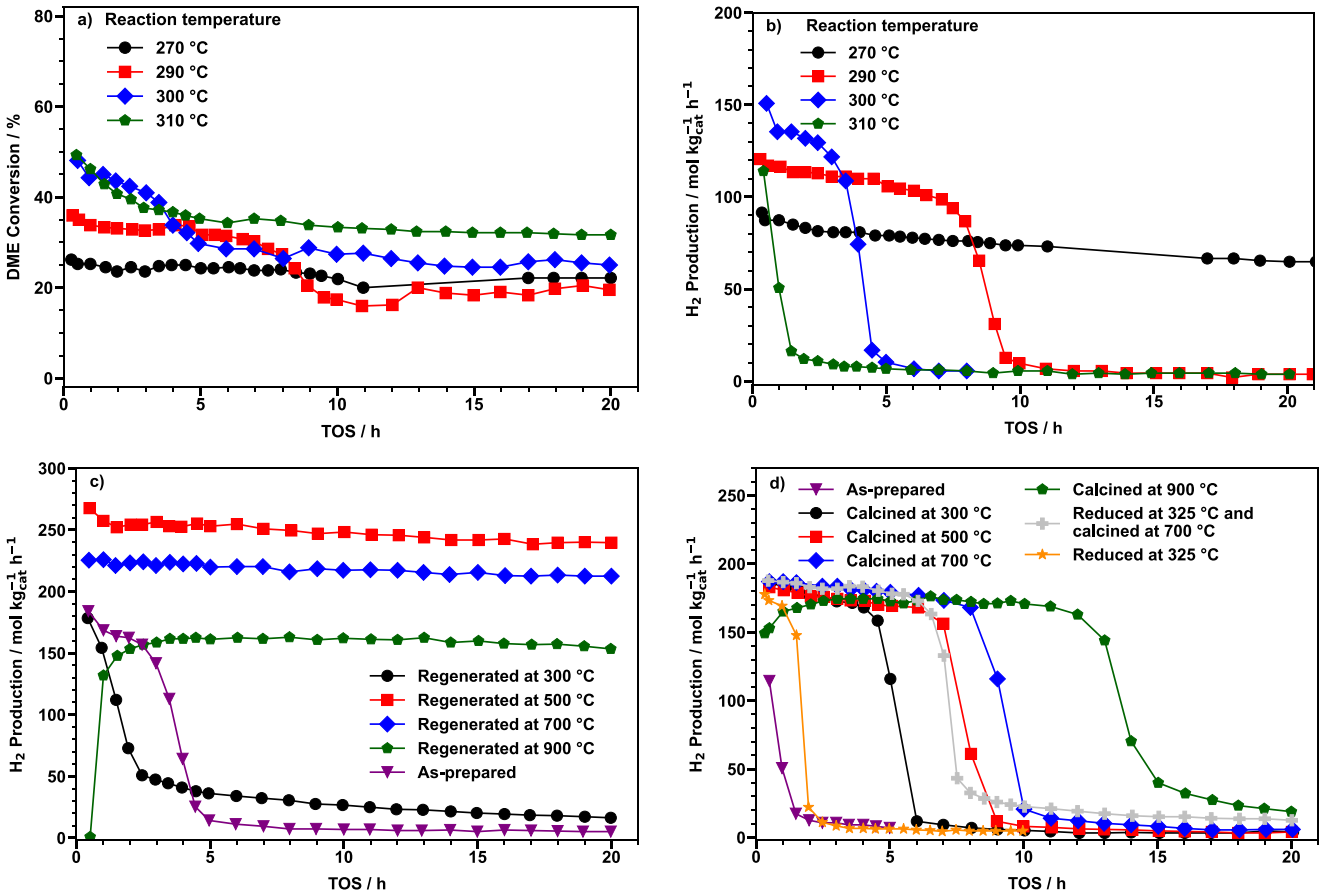

FIGURE 7 | Effect of regeneration and pretreatment conditions on the stability of $CuFe_2O_4$/ZSM-5 catalyst during DME SR. Trends on (a) DME conversion and (b) rate of H_2 production. (c) Rate of H_2 production at 300°C for 20 h after catalyst regeneration at higher temperatures. Adapted from Shimoda et al. Copyright (2010), Elsevier [56]. (d) Effect of thermal pretreatment on H_2 production at 325°C for 20 h. Adapted from Shimoda et al. Copyright (2011), Elsevier [53]. Reaction conditions: (a) and (b) 270°C–310°C, W/F = 5.0 g min L^{-1}, S/C = 2.5; (c) 300°C, W/F = 3.0 g min L^{-1}, and S/C = 2.5; and (d) 325°C, W/F = 5.0 g min L^{-1} and S/C = 2.5. Catalyst regeneration in air at 500°C and 700°C enhances activity and stability.

temperature (300°C vs. 325°C), catalyst mass, flow rates of the feed mixture, could influence catalyst performance and productivity. On the other hand, the timing of the heat treatment may play a critical role. In the earlier study, thermal treatment was employed after the catalyst test (as catalyst regeneration strategy), whereas in the study by Shimoda et al. (from 2011), the calcination was performed prior to the reaction (as catalyst pretreatment condition). The reaction conditions may have induced structural modifications in the catalyst, for instance, through a reduction in its acidity. This decrease in acidity could have contributed to enhanced catalyst stability following heat treatment compared to heat treatment alone. Furthermore, it is noteworthy that the initial H_2 production of the calcined bifunctional catalysts was very similar. However, as shown in Figure 7c, regeneration at 500°C and 700°C resulted in increased productivity thereafter. Additionally, the observation of catalyst deactivation when DME SR was performed at 325°C for all treatments did not result in deactivation over the same time period as performing DME SR at 300°C with similarly thermal-treated catalysts. This suggests that reaction temperatures above 300°C are not suitable for this catalyst system. Therefore, performing DME SR below 300°C appears more suitable for this catalyst system. However, for a more rigorous comparison between catalyst pretreatment and regeneration conditions, experiments should be conducted under identical reaction conditions, particularly at 300°C. This would minimize reaction temperature-dependent effects, such as enhanced hydrocarbon formation at higher temperatures, and allow clearer differentiation between the effects of pretreatment and regeneration on catalyst structure, activity, and stability. These two studies clearly show that catalyst stability can be improved by heat treatment, most likely due to the changes in acidity. The conditions and duration of the heat treatment can also affect the Cu-based catalyst required for the steam reforming step, as evidenced by the formation of small CuO grains in the $CuFe_2O_4$ catalyst after regeneration. However, the dynamics of the Cu-based catalyst in such bifunctional catalysts for DME SR remains insufficiently explored in the literature.

A ferrierite-based bifunctional catalyst was also calcined before performing DME SR to enhance stability. However, catalyst stability did not improve, likely attributed to the loss of its acid properties caused by the high thermal treatment. Moreover, the nature of carbon species deposited on both spent ferrierite-based and ZSM-5-based catalysts was different, indicating that the two zeolites possessed distinct acidic properties after the heat treatment [53]. The fact that the heat treatment of ferrierite did not improve catalyst stability implies that structural changes may have occurred during the heat treatment, thus altering the

amount and strength of the acidic sites. In particular, the decrease in H_2 production at 325°C for ferrierite-based bifunctional catalyst indicates the presence of high Brønsted acidity, which likely promoted rapid carbon deposition and subsequent catalyst deactivation. In contrast, the stable H_2 production observed for thermally treated ZSM-5 suggests that calcination may have reduced the acidity of critical active sites, thereby slowing carbon formation and improving stability. However, as the pretreated catalysts were not further characterized and reported, no direct evidence is available regarding changes in acidity, acid site distribution, or structural integrity.

The primary metal–zeolite bifunctional catalyst deactivation mechanism during DME SR is coke formation due to the high Brønsted acidity. Consequently, reducing zeolite acidity, either by lowering the concentration of Brønsted acid sites or decreasing their intrinsic acid strength, represents an effective strategy to mitigate catalyst deactivation. The above-mentioned studies tried to address this issue by applying heat treatment conditions before or after the DME SR. However, tailoring the zeolite prior to combining it with the copper-based reforming catalyst represents a more controlled and potentially more effective approach. For example, a recent study investigated ZSM-5 zeolite modified with La, Fe, Cu, and P, a decrease in acidity, as measured by NH_3-TPD, was observed compared to the untreated ZSM-5. Among the incorporated modifiers, the addition of La had the most pronounced effect on the acidity and showed a stable H_2 yield of 74% for 10 h TOS at 300°C. In comparison, the H_2 yield of untreated HZSM-5 significantly declined under identical experimental conditions [57]. This finding demonstrates that controlled tuning of zeolite acidity is a key parameter for improving catalyst stability in bifunctional catalysts for DME SR. Importantly, this approach allows suppression of coke formation while maintaining sufficient acidity for DME hydrolysis, highlighting the need for an optimal balance between catalyst activity and stability under longer TOS. The observation that both heat treatment and modification of ZSM-5 improve catalyst stability highlights acidity as a key parameter for tailoring stability. However, since heat treatment of ferrierite did not lead to a similar improvement, its overall impact should extend beyond the acidity alone. Effects on factors such as zeolite topology or copper dispersion need to be considered.

In addition to limiting coke formation, suppression of RWGS reaction is another important aspect of DME SR to enhance the H_2 yield, as it consumes H_2 and produces CO. Thermodynamic calculations by Semelsberger et al. (discussed above), showed that CO formation increases with temperature under stoichiometric conditions (i.e., S/C = 1.5), with CO fraction rising from 0.0260 at 200°C to 0.0571 at 300°C [36]. Increasing the S/C ratio to 3 significantly reduced the CO fraction to 0.0015 and 0.0081 at 200°C and 300°C, respectively, demonstrating the strong influence of steam partial pressure on suppressing the RWGS reaction. Experimental results reported by Tanaka et al. confirmed these thermodynamic trends [37]. Using a Cu–Mn–Fe spinel mixed with alumina as a bifunctional catalyst, an increasing CO selectivity was observed with increasing reaction temperature, but with increasing S/C ratio higher than the stoichiometric value CO selectivity declined. Also, higher space velocities reduced CO selectivity. Nevertheless, this benefit was accompanied by a decrease in DME conversion, illustrating a trade-off between conversion and selectivity. However, the catalyst should also be stable in harsh conditions with high water content, so that RWGS is suppressed, but the catalyst still remains active. The increase in CO formation with increasing reaction temperatures, due to the RWGS reaction, along with hydrocarbon formation on Brønsted acid sites of zeolites at temperatures of 300°C and above, is well discussed here and across the broader DME SR literature. These effects clearly limit DME SR operation to reaction temperatures below 300°C.

The studies on bifunctional catalyst stability and regeneration during DME SR highlight several important process and catalyst design considerations for efficient H_2 release. From the catalyst design side, the development of catalysts that are highly active for DME hydrolysis and steam reforming at low reaction temperatures is essential. In particular, optimizing the acid function of zeolites plays a key role, as Cu-based catalysts intrinsically catalyze both steam reforming and RWGS reactions, making the hydrolysis step a bottleneck for overall catalytic performance. From the operating condition and process perspective, reaction temperatures below 300°C and using an elevated S/C ratio are effective strategies to suppress dehydration and RWGS, thus minimizing hydrocarbons and CO formation. Furthermore, innovative reactor design can provide an additional means of CO transformation from the product stream. For instance, integrating a water–gas shift reactor has been shown to reduce CO concentration from the gas stream and increase H_2 yield, demonstrating the importance of combining catalyst and process optimization strategies [58].

In summary, the studies on bifunctional catalysts for DME SR demonstrated the potential of zeolites with rich topological structures and enhanced acidity as solid acid catalysts for the hydrolysis step. The advantage of zeolite-based solid acids includes high DME conversion that can be obtained at operating temperatures compatible with Cu-based catalysts, such as $Cu/ZnO/Al_2O_3$ catalyst (<300°C). This, in turn, helps to tackle the required higher temperature to obtain decent DME conversion (>300°C) when alumina is used as a solid acid, and the associated challenges, such as the deactivation of Cu-based catalyst due to sintering, a decreased H_2 yield with an increased CO formation due to RWGS reaction, and hydrocarbons as side products from DME decomposition, and so forth. Design rules for bifunctional catalysts for low-temperature DME steam reforming (200°C–300°C) require optimization of both the acidic and metallic functions, while ensuring hydrothermal and thermal stability. The hydrolysis of DME to methanol requires sufficient Brønsted acidity, typically provided by zeolites. Zeolites such as mordenite, ferrierite, and ZSM-5 have demonstrated high DME conversion below 300°C. While two-dimensional channel systems may enhance diffusion and site accessibility, pore architecture alone does not determine performance; acid strength, acid site amount, and accessibility need to be balanced. The methanol steam reforming step typically occurs over copper-based catalysts. So far, $CuFe_2O_4$ spinel-type catalysts achieved improved stability during longer TOS due to their resistance to sintering and structural degradation. Moreover, high S/C ratios are beneficial to suppress CO formation and enhance H_2 selectivity. Therefore, both components of the bifunctional catalyst should remain stable under high water fraction. On the contrary, strong Brønsted acid sites also promote hydrocarbon formation

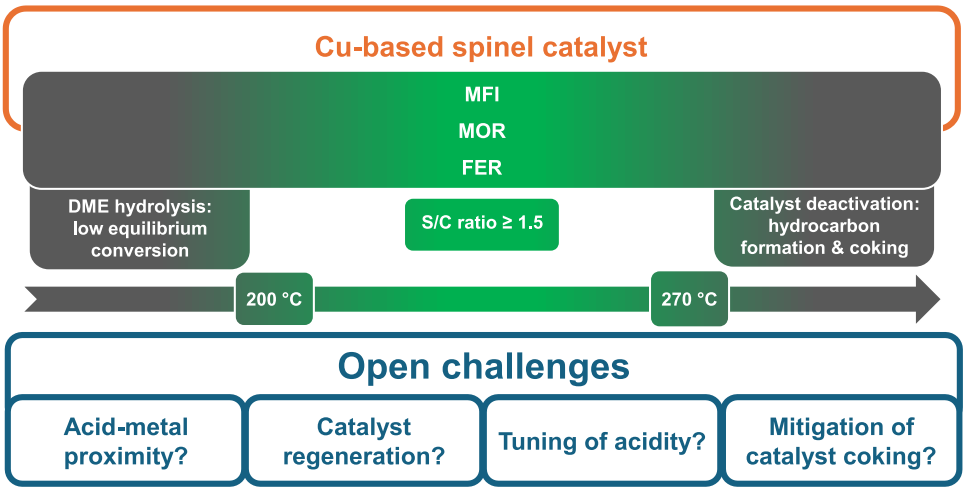

FIGURE 8 | Summary of optimal reaction conditions, catalyst classes, and open challenges for low-temperature DME SR. The optimal reaction temperature range is 200°C–270°C when using Cu-based spinels and zeolites such as ZSM-5, mordenite, or ferrierite. Lower reaction temperatures result in low DME conversion, while higher temperatures promote catalyst deactivation.

and coke deposition, leading to reduced H_2 yield and catalyst deactivation. Therefore, acidity must be optimized rather than maximized. Thermal stability during the bifunctional catalyst regeneration is also critical. Copper spinel catalysts, calcined at temperatures above 500°C, provide high structural stability. Similarly, the zeolite must retain crystallinity and acidity under hydrothermal and high-temperature regeneration conditions. Overall, the optimal bifunctional catalyst combines controlled Brønsted acidity for efficient DME hydrolysis with a thermally stable copper-based reforming catalyst, ensuring high hydrogen yield, low CO formation, and resistance to deactivation.

6 | Summary and Perspectives

DME is considered a viable H_2 carrier because of its high technical storage capacity of 26.1 wt.%, non-toxicity, and LPG-like properties. DME can be directly synthesized from CO_2 and H_2, and stored H_2 can be released through a steam reforming reaction with only CO_2 and H_2 as products. Both reactions involve two steps. For DME SR, DME is first hydrolyzed to methanol over an acid catalyst, and methanol is then steam reformed to CO_2 and H_2, most commonly over a Cu-based catalyst. Cu-based spinel-type catalysts provide enhanced thermal stability, and it is also possible to regenerate and even enhance H_2 production after heat treatment of the bifunctional catalyst. Since RWGS can also be catalyzed by Cu-based catalysts, CO is a common side-product of DME SR. Acid catalysts like alumina or zeolites can be used for both DME synthesis and DME SR. Zeolites have been demonstrated to be effective at temperatures below 300°C due to their Brønsted acidity. However, DME conversion during hydrolysis is limited by equilibrium, but mixing the hydrolysis catalyst with an efficient steam reforming catalyst allows higher DME conversion rates, even reaching full conversion at low reaction temperatures.

In Figure 8, the optimal reaction conditions for low-temperature DME SR and open challenges are summarized. Cu-based spinel catalyst showed good stability and zeolites of the MFI, mordenite and ferrierite type showed the best results for DME hydrolysis and DME SR between 200°C and 270°C. At temperatures > 270°C, catalyst deactivation due to hydrocarbon formation and subsequent coking occurred. At temperatures even lower than 200°C, a very low equilibrium conversion and reaction rate was observed. The still open challenges for low-temperature DME SR are the effect of the acid–metal proximity, regeneration strategies also at temperatures below 500°C, and the tuning of the acidity and other methods to mitigate catalyst coking and deactivation.

For low-temperature DME SR, using zeolites or other solid acids with high Brønsted acidity is necessary. However, at temperatures above 300°C, zeolites can also produce hydrocarbons and lead to CO formation via the RWGS reaction over the Cu-based catalysts. Hence, the type of zeolite used for DME hydrolysis is important for DME SR, as the acid amount and strength, as well as other physicochemical properties of the catalysts, influence both DME hydrolysis and the subsequent methanol steam reforming. To date, the research has focused on investigating various commercial zeolites with different Si/Al ratios, alumina and heteropoly acid, as acid functionalities in DME SR. Moreover, few studies have examined the effects of tailoring zeolites' acidity, optimizing reaction conditions (i.e., S/C ratio, temperature, GHSV), and developing catalyst regeneration strategies to achieve high catalytic performance and long-term stability. Considering the potential of low-temperature DME SR, the research will continue to evolve. Hence, to guide future research on the topic toward a more efficient and strategic rationalization of catalyst design, the following aspects are recommended:

1. Tailoring acidity of zeolites: Brønsted acidity is proven crucial for DME hydrolysis, but its amount and strength need to be controlled for efficient catalyst performance. This can be achieved by either adjusting the Si/Al ratio during the synthesis or post-synthesis treatments of commercial zeolites. Post-synthesis treatments of commercial zeolite are considered efficient strategies to tailor acidic sites and screen the effect of various parameters in a short time. These strategies include ion

exchange (both exchanging the zeolite's extra-framework cations or partial exchange with other metal cations), isomorphous substitution (replacing framework Al with other heteroatoms), as well as dealumination and desilication. It has been shown that the addition of metal oxides in the zeolite structure decreases the acidity and can improve the catalyst stability [57]. For the DME to olefins (DTO) process, passivation of zeolite surface has been investigated as a potential strategy to increase catalyst stability. A silicalite-1 layer has been successfully employed to cover the surface, blocking access to the acid sites and thereby reducing the zeolite acidity and coke deposition during the reaction [59]. Since the sites active for DTO are the same as those considered for DME hydrolysis, the same approach could also be used to enhance stability of DME SR catalysts. By applying such surface modification, the acidity of zeolites can be fine-tuned, enabling systematic evaluation of catalytic performance and product selectivity under thermodynamic constraints of DME hydrolysis. This approach allows not only investigation of the effects of reduced acidity, but also how different modes of acidity modification influence catalyst behavior. Importantly, this methodology not only allows evaluation of the effects of reducing acidity but also provides insight into how different modes of acidity modification (e.g., surface passivation vs. bulk alteration) impact reaction pathways and catalyst stability.

The acidity of the zeolite is not the only influence the zeolites have on DME SR. The possible effect of the hydrophobicity of zeolites on DME hydrolysis is also an open area of research that needs to be addressed. An improved water adsorption capacity of zeolites could enhance the DME hydrolysis step. Also, in regard to zeolites, the effect of the pore structure, especially the pore topology and diffusion of DME, water and methanol through the pore system, is a factor often overlooked in literature. For example, diffusion through the zeolite pores could be investigated using quasi-elastic neutron scattering (QENS) or pulsed field gradient nuclear magnetic resonance (PFG NMR) [60, 61].

2. Optimizing Cu-based catalysts: So far, Cu-based catalysts are considered a good choice for methanol steam reforming with the advantages of cost-effectiveness, low-temperature activity, and high H_2 selectivity. Most studies reported in the literature focused on either tuning Cu crystal structure or doping other metals, such as Fe, Ni, and Co, to enhance catalytic performance. However, the fundamental issues, such as identifying the active sites and elucidating the reaction mechanism, have not been properly addressed due to the complex catalyst structure and involved reaction steps. Hence, a careful catalyst design with reduced system complexity is still required to understand the underlying parameters and develop an optimized catalyst. This can be achieved by optimizing the redox properties of Cu sites to obtain a balanced Cu^0–Cu^+ ratio, tailoring the metal–support interaction, and investigating the exsolution behavior of Cu sites from spinel-type or mixed oxide phases. It has been shown that both Cu^0 and Cu^+ are active species for methanol steam reforming [62], but the interplay between these two species is not understood. If both species are necessary for steam reforming, the stabilization of the Cu^+ species is imperative for a highly active catalyst. Polyhedral CeO_2 was able to stabilize Cu^+ species, also because of the high density of oxygen vacancies in its structure [63]. The doping of methanol steam reforming catalysts with Ce and the introduction of oxygen vacancies might lead to stabilized Cu^0 and Cu^+ species and, therefore, activity and stability might be improved.

Moreover, deactivation of the Cu-based catalyst, particularly through sintering, needs to be carefully considered, along with the interactions between the acid component and the Cu-based catalyst during DME SR. As described earlier, physically mixing Cu catalysts with zeolites can alter the reduction behavior and dispersion of copper species, which in turn affects catalytic activity and stability. Consequently, optimizing the Cu-based catalyst solely for the methanol SR step is insufficient. Instead, the entire catalytic system must be evaluated holistically, taking into account metal–acid interactions, structural stability under reaction conditions, and the dynamic changes that occur during operation. Such an integrated approach is essential to achieving both high performance and long-term stability in DME SR.

3. Effect of the proximity of the two functionalities: To understand and clarify the advantages of different configurations of the individually optimized functionalities, the influence of proximity between both optimized Cu-based catalyst and zeolite on product distribution should be studied by applying different spatial distributions of these functionalities within the catalytic bed. Different strategies, including a dual bed configuration, mechanical mixing and grinding (for better spatial proximity of these two components), as well as dispersing Cu nanoparticles on the zeolites, can be investigated. A double layered catalytic bed separates both catalysts on a macroscopic scale, and the physical mixing of both catalysts brings them closer together. In the case of mixing powders on a macroscopic scale, both catalysts are one material, but the functionalities are still separated. In a catalyst bed with an impregnated catalyst (e.g., copper impregnated on zeolite), both catalytic functionalities are on the same material and no longer separated. It has been shown that, for the non-oxidative methanol conversion into dimethoxymethane, the proximity between the Cu- and acid components was essential for achieving enhanced product selectivity. A dual-bed configuration favored the formation of methyl formate, while simple physical mixing of the two components resulted in only limited dimethoxymethane formation. In contrast, dispersing Cu particles onto the zeolite significantly enhanced dimethoxymethane selectivity [64]. As the catalyst components as well as substrates, products and potential side products in this reaction are closely similar to those in DME-SR, a similar dependence of conversion and selectivity on metal–acid proximity can be expected. Moreover, such studies provide a framework for evaluating whether a configuration with the closest proximity facilitates faster diffusion of reactive intermediates between active sites. This could, in turn, enhance reaction kinetics and promote the selective formation of H_2 and CO_2 by minimizing the accumulation of undesired intermediates and side reactions.

4. Operando and mechanistic investigations: As mentioned above, current catalyst development for DME SR lacks clarity on the state of the Cu active sites and reaction mechanism. Therefore, comprehensive operando investigations combining spatially and temporally resolved operando characterization (i.e., operando DRIFTS, XPS, and EXAFS), kinetic studies, and atomic simulations (computational studies) are crucial to unravel the nature of active sites, establish structure–activity relationships,

and elucidate the reaction mechanism. Gaining these fundamental insights will not only provide rational guidelines for designing optimized DME SR catalysts but also accelerate the practical implementation of the technology. However, considering the complexity of the bifunctional catalyst and the various reaction networks involved, it is suggested to first study separately the dynamics of the acid sites of the zeolites during DME hydrolysis and the evolution of the different Cu species during methanol steam reforming using operando techniques. For example, XANES spectroscopy can be used to determine oxidation state and coordination of Cu during methanol steam reforming [65]. But also, the oxidation state and coordination of other added metals like Zn in the $Cu/ZnAl_2O_4$ catalyst or the addition of Ce can be investigated, and the results used to optimize the metal ratio.

5. Optimizing reaction conditions: Product distribution and DME conversion during DME SR are dependent on the reaction conditions employed, such as S/C ratio, gas hourly space velocity (GHSV), temperature, and pressure, and so forth. Therefore, along with testing the newly designed catalysts under stochiometric ratios and standard reaction temperatures, it is crucial to evaluate catalytic performance under a wide range of reaction conditions. Such an approach will help to benchmark catalyst performance across different parameters and establish a catalyst portfolio that clearly highlights the advantages and limitations of each material. The optimal temperature range for zeolites to mitigate coking seemed to be between 200°C and 270°C with S/C ratio higher than the stoichiometric value of 1.5. However, the tuning of the zeolites' acidity can also reduce coking; therefore, the S/C ratio needs to be adjusted as well. Since a higher GHSV also has a negative influence on DME conversion but reduces CO selectivity, a study combining these optimized reaction conditions is crucial.

6. Long-term stability and catalyst regeneration strategies: To implement the newly developed catalysts in practical DME SR application, catalyst stability should be maintained for long-term time on stream (1000 h). Catalyst stability has to be evaluated not only under stochiometric conditions but also under various temperatures (especially thermal cycling), pressures, GHSVs, and S/C ratios to facilitate catalyst aging and deactivation. Moreover, catalyst stability should also be investigated under reduced DME conversions to ensure that deactivation is not hidden by a surplus of active sites in the presence of a high catalyst amount and less harsh reaction conditions. Tuning of the acidity has been shown to be beneficial for the catalyst stability, because the main deactivation mechanism for the bifunctional catalyst was coke deposition due to the zeolites' acidity. The acidity of the zeolites could be reduced by adding metal oxides to the zeolites, for example, by adding La or Fe onto the zeolite by impregnating and subsequent calcination [57]. However, the deactivation of the Cu-based catalyst, either by coke (from the zeolite), sintering or clustering of Cu particles, or Cu oxidation due to the harsh conditions, a high S/C ratio cannot be ignored. The stability of the Cu-based catalyst could be increased by doping a Cu-based spinel with other metals like Pd [66].

If catalyst deactivation is unavoidable, the development of innovative and more efficient regeneration strategies will play a significant role in designing optimized catalysts. The potential of regeneration strategies, such as thermal treatment and re-reduction, can be evaluated to restore the catalytic performance of deactivated catalysts. In this article, regeneration at high temperatures above 500°C was shown to be successful, but repeated regeneration cycles at these high temperatures could have a negative effect on the catalyst, be it acidity or pore structure. The development of regeneration strategies at lower temperatures would open the door for a catalyst that can be regenerated repeatedly without losing activity. Moreover, following the structural dynamics operando and performing post-reaction characterization facilitates understanding of the changes that occurred during deactivation, and guides the development of efficient regeneration strategies. With these understandings, regeneration strategies that employ only mild conditions and possibly a temperature of around 300°C. It was found that ozone at 450°C–500°C was able to remove coke from zeolites, but also the regeneration of coked zeolites by a discharge of non-thermal plasma was possible [67, 68]. These regeneration strategies might have worked for pure zeolites; still, the effect of such methods on the Cu-based catalyst also needs to be studied to employ them for bifunctional DME SR catalyst.

Overall, while low-temperature DME SR is still in an early research phase, its potential benefits are anticipated to surpass the associated challenges. Current difficulties with respect to catalyst development for low-temperature DME SR include achieving high activity, low CO formation, and stable performance over an extended time on stream. We believe that further research on target-based catalyst design will help advance promising laboratory results into robust commercial-scale low-temperature DME SR technologies.

Acknowledgments

The authors acknowledge the funding by the German Federal Ministry of Research, Technology and Space (BMFTR) and the Ministry of Economic Affairs, Industry, Climate Action and Energy of the State of North Rhine-Westphalia through the project HC-H2. This work was also supported by the Cluster of Excellence Fuel Science Center (EXC 2186, ID: 390919832) funded by the Excellence Initiative by the German federal and state governments to promote science and research at German universities.

Conflicts of Interest

The authors declare no conflicts of interest.

Declaration of Generative AI and AI-Assisted Technologies in the Writing Process

Generative AI was used to help generating and debugging code for the creation of most figures.

References

1. IPCC, "Section 2: Current Status and Trends," In Climate Change 2023: Synthesis Report, Contribution of Working Groups I, II and III to the Sixth Assessment Report of the Intergovernmental Panel on Climate Change, Core Writing Team, ed. H. Lee and J. Romero (IPCC, 2023), 41–66.

2. Z. Deng, B. Zhu, S. J. Davis, et al., "Global Carbon Emissions and Decarbonization in 2024," *Nature Reviews Earth & Environment* 6 (2025): 231–233.

3. N. I. Badea, "Hydrogen as Energy Sources—Basic Concepts," *Energies* 14 (2021): 5783.

4. P. Schühle, R. Stöber, M. Semmel, et al., "Dimethyl Ether/CO_2 – a Hitherto Underestimated H_2 Storage Cycle," *Energy & Environmental Science* 16 (2023): 3002–3013.

5. A. Godula-Jopek, W. Jehle, and J. Wellnitz, In *Hydrogen Storage Technologies: New Materials, Transport and Infrastructure* (Wiley, 2012), 97–170.

6. F. Dalena, A. Senatore, A. Marino, A. Gordano, M. Basile, and A. Basile, in *Methanol*, ed. A. Basile and F. Dalena (Elsevier, 2018), 3–28.

7. E. Catizzone, C. Freda, G. Braccio, F. Frusteri, and G. Bonura, "Dimethyl Ether as Circular Hydrogen Carrier: Catalytic Aspects of Hydrogenation/Dehydrogenation Steps," *Journal of Energy Chemistry* 58 (2021): 55–77.

8. J. Wu, Z. Liu, J. Pan, and X. Zhao, "Vapor Pressure Measurements of Dimethyl Ether From (233 to 399) K," *Journal of Chemical and Engineering Data* 49 (2004): 32–34.

9. T. A. Semelsberger, R. L. Borup, and H. L. Greene, "Dimethyl Ether (DME) as an Alternative Fuel," *Journal of Power Sources* 156 (2006): 497–511.

10. T. A. Semelsberger, K. C. Ott, R. L. Borup, and H. L. Greene, "Generating Hydrogen-Rich Fuel-Cell Feeds From Dimethyl Ether (DME) Using Cu/Zn Supported on Various Solid-Acid Substrates," *Applied Catalysis A: General* 309 (2006): 210–223.

11. R. González-Gil, P. Kowalik, K. Antoniak-Jurak, et al., "The Role of Lewis Acidic Vanadium Centers in DME Steam Reforming Over V–Ni Catalysts," *Chemical Engineering Journal* 423 (2021): 129996.

12. C. Kim, B. Choi, and K. Lee, "Hydrogen Generation Characteristics of Reduced DME Steam Reforming Catalysts According to Heating Methods," *International Journal of Hydrogen Energy* 47 (2022): 36058–36072.

13. J. O. Ighalo and A. G. Adeniyi, "Thermodynamic Modelling of Dimethyl Ether Steam Reforming," *Clean Technologies and Environmental Policy* 23 (2021): 1353–1363.

14. C. T. Rodrigues, G. F. de Lopes, T. L. de Souza, L. M. M. de Jorge, and P. R. Paraíso, "Methanol and Dimethyl Ether Steam Reforming: A Thermodynamic Analysis," *Brazilian Journal of Chemical Engineering* 40 (2022): 885–899.

15. T.-Q. Zhang, B. Choi, and Y.-B. Kim, "Numerical and Experimental Study on Hydrogen Production Via Dimethyl Ether Steam Reforming," *International Journal of Hydrogen Energy* 45 (2020): 11438–11448.

16. S. Wei and C. Li, "Design and Optimization of Spiral Heated Tubular Dimethyl Ether (DME) Steam Reforming Reactor," *International Journal of Hydrogen Energy* 48 (2023): 2231–2246.

17. D. Kim, B. Choi, G. Park, K. Lee, D.-W. Lee, and S. Jung, "Effect of γ-Al_2O_3 Characteristics on Hydrogen Production of Cu/γ-Al_2O_3 Catalyst for Steam Reforming of Dimethyl Ether," *Chemical Engineering Science* 216 (2020): 115535.

18. S.-S. Wang, Y.-H. Song, Y.-H. Zhao, et al., "Amorphous Silica-Alumina Composite With Regulated Acidity for Efficient Production of Hydrogen Via Steam Reforming of Dimethyl Ether," *Catalysis Today* 351 (2020): 68–74.

19. R. Stöber, F. Seidl, E. Hoffmann, P. Wasserscheid, and P. Schühle, "A Highly Durable Catalyst System for Hydrogen Production From Dimethyl Ether," *Sustainable Energy Fuels* 8 (2024): 1740–1749.

20. R. Zhang, Z. Ni, J. Li, et al., "Catalysts for Dimethyl Ether Reforming to Hydrogen (A Review)," *Russian Journal of General Chemistry* 94 (2024): 690–702.

21. S. P. Naik, T. Ryu, V. Bui, J. D. Miller, N. B. Drinnan, and W. Zmierczak, "Synthesis of DME From CO_2/H_2 Gas Mixture," *Chemical Engineering Journal* 167 (2011): 362–368.

22. S. Ren, W. R. Shoemaker, X. Wang, et al., "Highly Active and Selective Cu-ZnO Based Catalyst for Methanol and Dimethyl Ether Synthesis via CO_2 Hydrogenation," *Fuel* 239 (2019): 1125–1133.

23. S. Wang, D. Mao, X. Guo, G. Wu, and G. Lu, "Dimethyl Ether Synthesis via CO2 Hydrogenation Over CuO–TiO_2–ZrO_2/HZSM-5 Bifunctional catalysts," *Catalysis Communications* 10 (2009), 1367–1370.

24. W. Kriprasertkul, T. Witoon, and P. Kim-Lohsoontorn, "Dimethyl Ether (DME) Synthesis From CO_2 and H_2 Through Ethanol-Assisted Methanol Synthesis and Methanol Dehydration," *International Journal of Hydrogen Energy* 47 (2022): 33338–33351.

25. G. Bonura, M. Cordaro, C. Cannilla, et al., "Catalytic Behaviour of a Bifunctional System for the One Step Synthesis of DME by CO_2 Hydrogenation," *Catalysis Today* 228 (2014): 51–57.

26. G. Bonura, M. Cordaro, L. Spadaro, C. Cannilla, F. Arena, and F. Frusteri, "Hybrid Cu–ZnO–ZrO_2/H-ZSM5 System for the Direct Synthesis of DME by CO_2 Hydrogenation," *Applied Catalysis B: Environmental* 140–141 (2013): 16–24.

27. N. S. Altinsoy and A. K. Avci, "Sorption Enhanced DME Synthesis by One-Step CO_2 Hydrogenation," *Chemical Engineering and Processing: Process Intensification* 203 (2024): 109874.

28. R. Liu, X. Shao, C. Wang, W. Dai, and N. Guan, "Reaction Mechanism of Methanol-to-Hydrocarbons Conversion: Fundamental and Application," *Chinese Journal of Catalysis* 47 (2023): 67–92.

29. N. Simitsis, C. Mebrahtu, and R. Palkovits, "Non-Oxidative Conversion of Methanol to Dimethyl Ether, Methyl Formate and Dimethoxymethane Over Cu/Hβ Catalyst: Tailoring Product Selectivity," *ChemCatChem* 16 (2024): e202301704.

30. S.-I. Fujita, M. Usui, and N. Takezawa, "Mechanism of the Reverse Water Gas Shift Reaction Over Cu/ZnO Catalyst," *Journal of Catalysis* 134 (1992): 220–225.

31. C.-S. Chen, W.-H. Cheng, and S.-S. Lin, "Study of Iron-Promoted Cu/SiO_2 Catalyst on High Temperature Reverse Water Gas Shift Reaction," *Applied Catalysis A: General* 257 (2004): 97–106.

32. K. Faungnawakij, Y. Tanaka, N. Shimoda, T. Fukunaga, R. Kikuchi, and K. Eguchi, "Hydrogen Production From Dimethyl Ether Steam Reforming Over Composite Catalysts of Copper Ferrite Spinel and Alumina," *Applied Catalysis B: Environmental* 74 (2007): 144–151.

33. P. Pérez-Uriarte, A. Ateka, M. Gamero, A. T. Aguayo, and J. Bilbao, "Effect of the Operating Conditions in the Transformation of DME to Olefins Over a HZSM-5 Zeolite Catalyst," *Industrial & Engineering Chemistry Research* 55 (2016): 6569–6578.

34. L. Oar-Arteta, A. T. Aguayo, A. Remiro, A. Arandia, J. Bilbao, and A. G. Gayubo, "Kinetics of the Steam Reforming of Dimethyl Ether Over $CuFe_2O_4$/γ-Al_2O_3," *Chemical Engineering Journal* 306 (2016): 401–412.

35. D. Feng, Y. Wang, D. Wang, and J. Wang, "Steam Reforming of Dimethyl Ether Over CuO–ZnO–Al_2O_3–ZrO_2+ZSM-5: A Kinetic Study," *Chemical Engineering Journal* 146 (2009): 477–485.

36. T. A. Semelsberger and R. L. Borup, "Thermodynamic Equilibrium Calculations of Dimethyl Ether Steam Reforming and Dimethyl Ether Hydrolysis," *Journal of Power Sources* 152 (2005): 87–96.

37. Y. Tanaka, R. Kikuchi, T. Takeguchi, and K. Eguchi, "Steam Reforming of Dimethyl Ether Over Composite Catalysts of γ-Al_2O_3 and Cu-Based Spinel," *Applied Catalysis B: Environmental* 57 (2005): 211–222.

38. M. Smyrnioti and T. Ioannides, "Dimethyl Ether Hydrolysis Over WO_3/γ-Al_2O_3 Supported Catalysts," *Catalysts* 12 (2022): 396.

39. G. L. Woolery, G. H. Kuehl, H. C. Timken, A. W. Chester, and J. C. Vartuli, "On the Nature of Framework Brønsted and Lewis Acid Sites in ZSM-5," *Zeolites* 19 (1997): 288–296.

40. S. Namuangruk, J. Meeprasert, P. Khemthong, and K. Faungnawakij, "A Combined Experimental and Theoretical Study on the Hydrolysis of Dimethyl Ether Over H-ZSM-5," *Journal of Physical Chemistry C* 115 (2011): 11649–11656.

41. J. Topp-Jørgensen, in *Stud. Surf. Sci. Catal., vol. 36*, ed. D. M. Bibby, C. D. Chang, R. F. Howe, S. Yurchak (Elsevier, 1988), 293–305.

42. P. Tian, Y. Wei, M. Ye, and Z. Liu, "Methanol to Olefins (MTO): From Fundamentals to Commercialization," *ACS Catalysis* 5 (2015): 1922–1938.

43. K. Chen, J. Kelsey, J. L. White, L. Zhang, and D. Resasco, "Water Interactions in Zeolite Catalysts and Their Hydrophobically Modified Analogues," *ACS Catalysis* 5 (2015): 7480–7487.

44. L. Shirazi, E. Jamshidi, and M. R. Ghasemi, "The Effect of Si/Al Ratio of ZSM-5 Zeolite on Its Morphology, Acidity and Crystal Size," *Crystal Research and Technology* 43 (2008): 1300–1306.

45. T. A. Semelsberger, K. C. Ott, R. L. Borup, and H. L. Greene, "Role of Acidity on the Hydrolysis of Dimethyl Ether (DME) to Methanol," *Applied Catalysis B: Environmental* 61 (2005): 281–287.

46. K. Faungnawakij, Y. Tanaka, N. Shimoda, et al., "Influence of Solid–Acid Catalysts on Steam Reforming and Hydrolysis of Dimethyl Ether for Hydrogen Production," *Applied Catalysis A: General* 304 (2006): 40–48.

47. V. Sanchez Escribano, G. Garbarino, E. Finocchio, and G. Busca, "γ-Alumina and Amorphous Silica–Alumina: Structural Features, Acid Sites and the Role of Adsorbed Water," *Topics in Catalysis* 60 (2017): 1554–1564.

48. P. Hirunsit, K. Faungnawakij, S. Namuangruk, and C. Luadthong, "Catalytic Behavior and Surface Species Investigation Over γ-Al_2O_3 in Dimethyl Ether Hydrolysis," *Applied Catalysis A: General* 460–461 (2013): 99–105.

49. L. B. M. Christian Baerlocher, D. Brouwer, and B. Marler, "Database of Zeolite Structures," accessed January 28, 2026, https://www.iza-structure.org/databases/.

50. S. Lin, Y. Zhi, Z. Liu, et al., "Multiscale Dynamical Cross-Talk in Zeolite-Catalyzed Methanol and Dimethyl Ether Conversions," *National Science Review* 9 (2022): nwac151.

51. A. Jentys, G. Warecka, M. Derewinski, and J. A. Lercher, "Adsorption of Water on ZSM 5 Zeolites," *Journal of Physical Chemistry* 93 (1989): 4837–4843.

52. D. H. Olson, W. O. Haag, and W. S. Borghard, "Use of Water as a Probe of Zeolitic Properties: Interaction of Water With HZSM-5," *Microporous and Mesoporous Materials* 35–36 (2000): 435–446.

53. N. Shimoda, K. Faungnawakij, R. Kikuchi, and K. Eguchi, "A Study of Various Zeolites and $CuFe_2O_4$ Spinel Composite Catalysts in Steam Reforming and Hydrolysis of Dimethyl Ether," *International Journal of Hydrogen Energy* 36 (2011): 1433–1441.

54. V. V. Galvita, G. L. Semin, V. D. Belyaev, T. M. Yurieva, and V. A. Sobyanin, "Production of Hydrogen From Dimethyl Ether," *Applied Catalysis A: General* 216 (2001): 85–90.

55. S. Kameoka, T. Tanabe, and A. P. Tsai, "Spinel $CuFe_2O_4$: A Precursor for Copper Catalyst With High Thermal Stability and Activity," *Catalysis Letters* 100 (2005): 89–93.

56. N. Shimoda, K. Faungnawakij, R. Kikuchi, and K. Eguchi, "Degradation and Regeneration of Copper-Iron Spinel and Zeolite Composite Catalysts in Steam Reforming of Dimethyl Ether," *Applied Catalysis A: General* 378 (2010): 234–242.

57. S.-H. Zhang, Y. H. Zhao, J.-K. Zhang, X.-Q. Feng, Q. J. Zhang, and H. Wang, "Oxide-Modified HZSM-5 for Efficient Production of Hydrogen Via Steam Reforming of Dimethyl Ether," *Research on Chemical Intermediates* 50 (2024): 3223–3237.

58. S.-J. Park, D.-W. Lee, C.-Y. Yu, K.-Y. Lee, and K.-H. Lee, "Hydrogen Production From a DME Reforming-Membrane Reactor Using Stainless Steel-Supported Knudsen Membranes With High Permeability," *Journal of Membrane Science* 318 (2008): 123–128.

59. E. Giglio, G. Ferrarelli, F. Salomone, et al., "Tailoring the Acidity of ZSM-5 Via Surface Passivation: Catalytic Assessment on Dimethyl Ether to Olefins (DTO) Process," *Fuel* 362 (2024): 130559.

60. H. Jobic, "Diffusion Studies Using Quasi-Elastic Neutron Scattering," *Membrane Science and Technology* 6 (2000): 109–137.

61. K. S. Han, J. D. Bazak, Y. Chen, et al., "Pulsed Field Gradient Nuclear Magnetic Resonance and Diffusion Analysis in Battery Research," *Chemistry of Materials* 33 (2021): 8562–8590.

62. K.-L. Chiu, F.-L. Kwong, and D. H. L. Ng, "Oxidation States of Cu in the $CuO/CeO_2/Al_2O_3$ Catalyst in the Methanol Steam Reforming Process," *Current Applied Physics* 12 (2012): 1195–1198.

63. Y. Gong, L. Hu, and Y. Zhou, "Morphology-Dependent Cu+ Stabilization and Metal–Support Interactions Govern Catalytic Transfer Hydrogenation of Furfural Over Cu/CeO_2," *Inorganic Chemistry* 64 (2025): 21971–21982.

64. R. Sun, C. Mebrahtu, J. P. Hofmann, et al., "Hydrogen-Efficient Non-Oxidative Transformation of Methanol Into Dimethoxymethane Over a Tailored Bifunctional Cu Catalyst," *Sustainable Energy Fuels* 5 (2021): 117–126.

65. C. Lamberti, S. Bordiga, F. Bonino, et al., "Determination of the Oxidation and Coordination state of Copper on Different Cu-Based Catalysts by XANES Spectroscopy In Situ or In Operando Conditions," *Physical Chemistry Chemical Physics* 5 (2003): 4502–4509.

66. K. Nomoto, Y. Kubo, H. Miura, and T. Shishido, "Production of Hydrogen by the Autothermal Reforming of Methanol Over $Cu/ZnO/Al_2O_3$-Based Catalysts: Improved Durability and Self-Activation Ability Upon Pd-Doping," *Journal of the Japan Petroleum Institute* 65 (2022): 161–170.

67. G. J. Hutchings, R. G. Copperthwaite, T. Themistocleous, et al., "A Comparative Study of Reactivation of Zeolite Y Using Oxygen and Ozone/Oxygen Mixtures," *Applied Catalysis* 34 (1987): 153–161.

68. L. Y. Jia, A. Farouha, L. Pinard, et al., "New Routes for Complete Regeneration of Coked Zeolite," *Applied Catalysis B: Environmental* 219 (2017): 82–91.

Biographies

Nick Heiming studied chemistry at RWTH Aachen University and received his master's degree in 2024 under supervision of Prof. R. Palkovits, focusing on DME steam reforming over bifunctional catalysts containing copper-based spinels and zeolites. In 2025, he joined the Institute for a Sustainable Hydrogen Economy of Forschungszentrum Jülich and continued his research on DME steam reforming for his doctoral studies under the supervision of Prof. R. Palkovits.

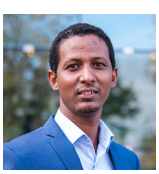

Chalachew Mebrahtu finished his Erasmus Mundus Joint PhD (SINCHEM) from the University of Messina and RWTH Aachen University (2018). Currently, he is a team leader with Prof. Regina Palkovits at the Institute for a Sustainable Hydrogen Economy, Research Center Jülich and group leader at RWTH Aachen University. His research focuses on the design of catalysts for sustainable H_2 storage, and the conversion of CO_2 and H_2O to synthetic fuels/chemicals.

Regina Palkovits is a full professor for heterogeneous catalysis and chemical technology at RWTH Aachen University and director of the Institute for a Sustainable Hydrogen Economy at Forschungszentrum Jülich. She graduated in chemical engineering from Technical University Dortmund and finished her PhD with Prof. Ferdi Schüth at the Max-Planck-Institut für Kohlenforschung. She received numerous awards, including the 2019 EFCATS Young Researcher Award and the 2016 DECHEMA Award. She is a Max Planck Fellow at the Max Planck Institute for Chemical Energy Conversion and as of 2020, a member of the North Rhine-Westphalian Academy of Sciences, Humanities and the Arts.